



Photometric BAO Measurements with DES

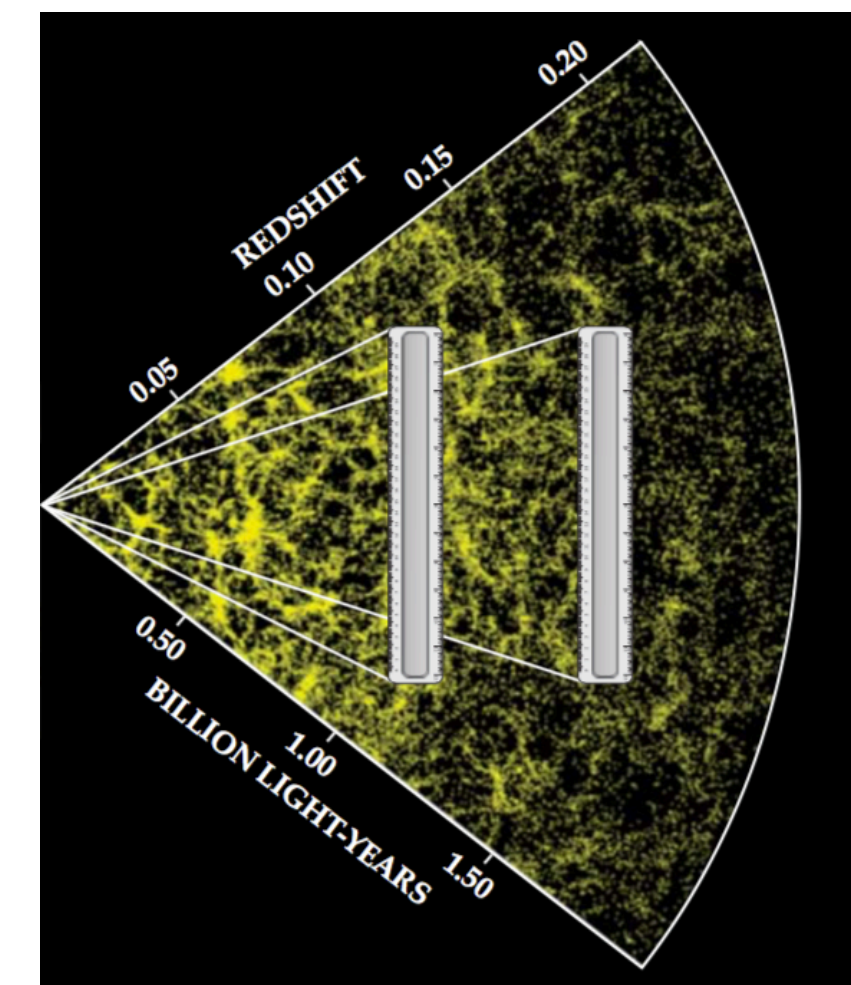
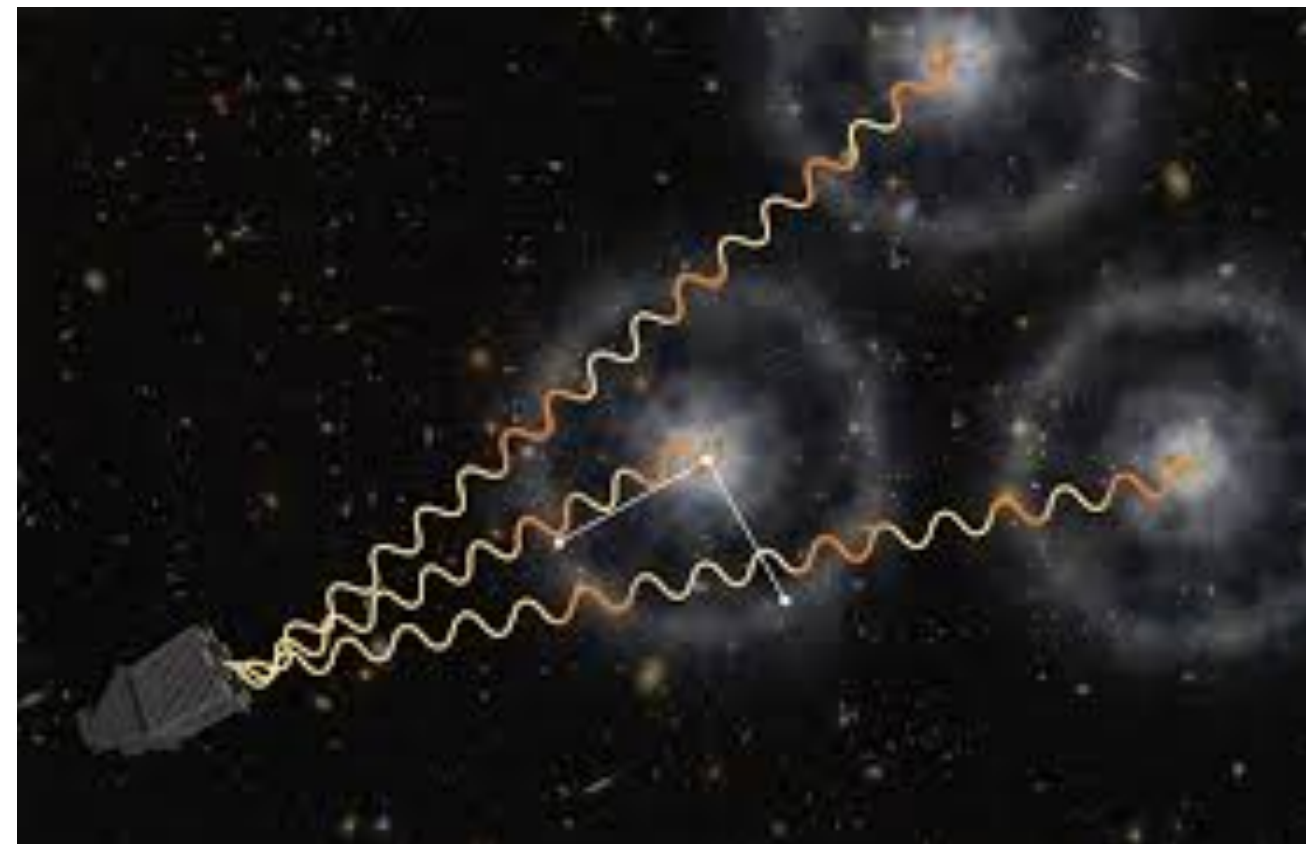
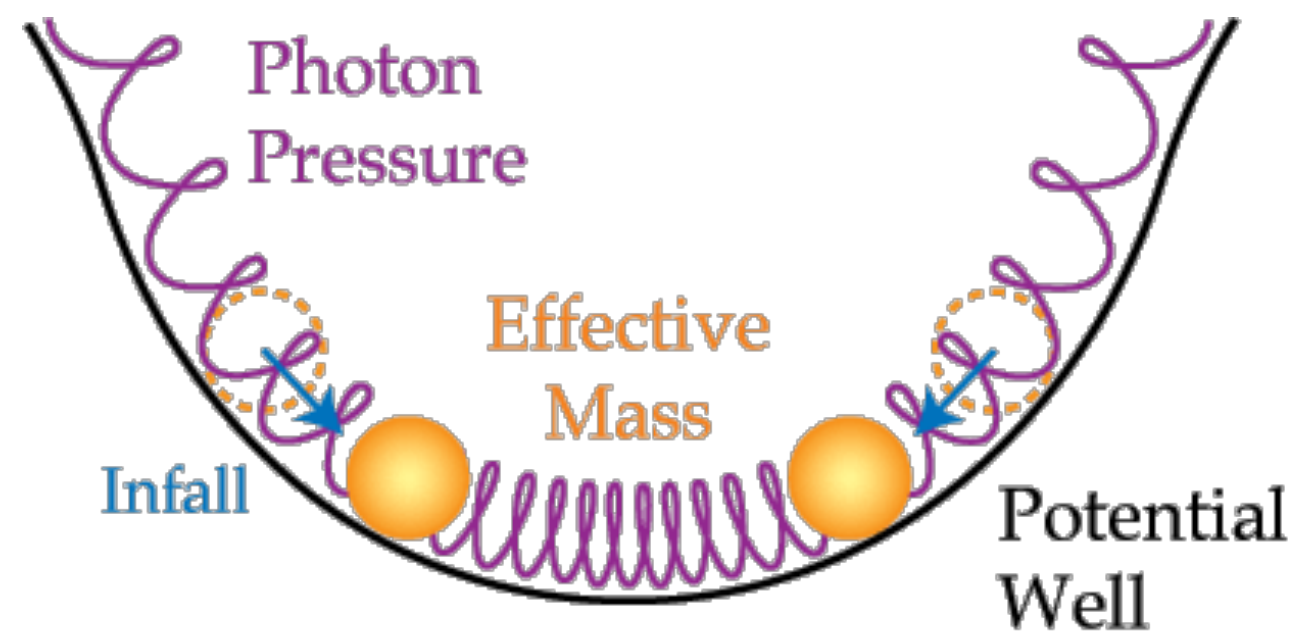
Kwan Chan Chan
Sun-Yat Sen University

In collaboration with DES BAO working group

The 32nd Texas Symposium on Relativistic Astrophysics
Shanghai, 14 Dec 2023

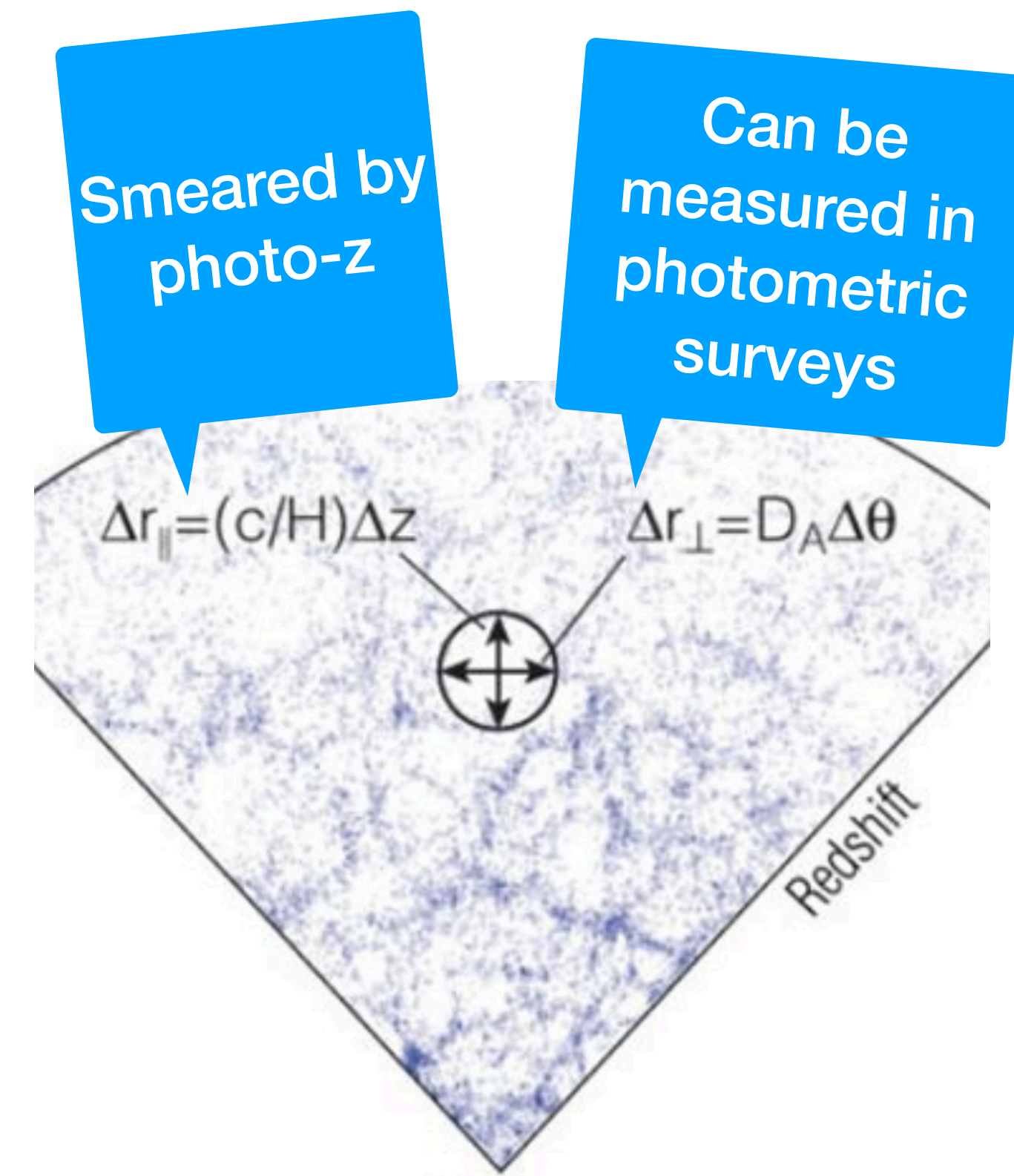
Baryonic Acoustic Oscillations (BAO)

- BAO is the imprint of the acoustic oscillations during the early universe in the distribution of the large-scale structure
- Provides a standard ruler in the late universe
- Has been measured in numerous analyses, most of them are based on spectroscopic data



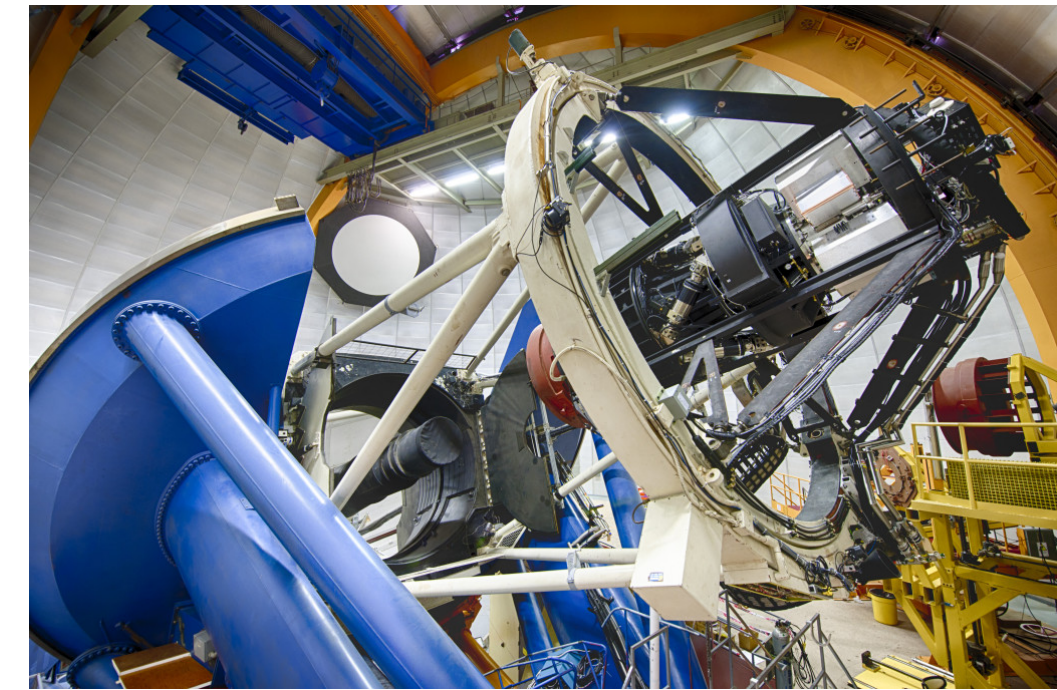
Photometric BAO

- Photometric surveys, lack of precise radial info, the radial BAO is smeared out, transverse BAO can be measured.
- The transverse BAO can be measured using the photometric data, and hence constraint on D_M/r_s
- Lots of photometric data from current and future imaging surveys, DES, HSC, KiDS, LSST, Euclid, CSST...





Dark Energy Survey Year 6

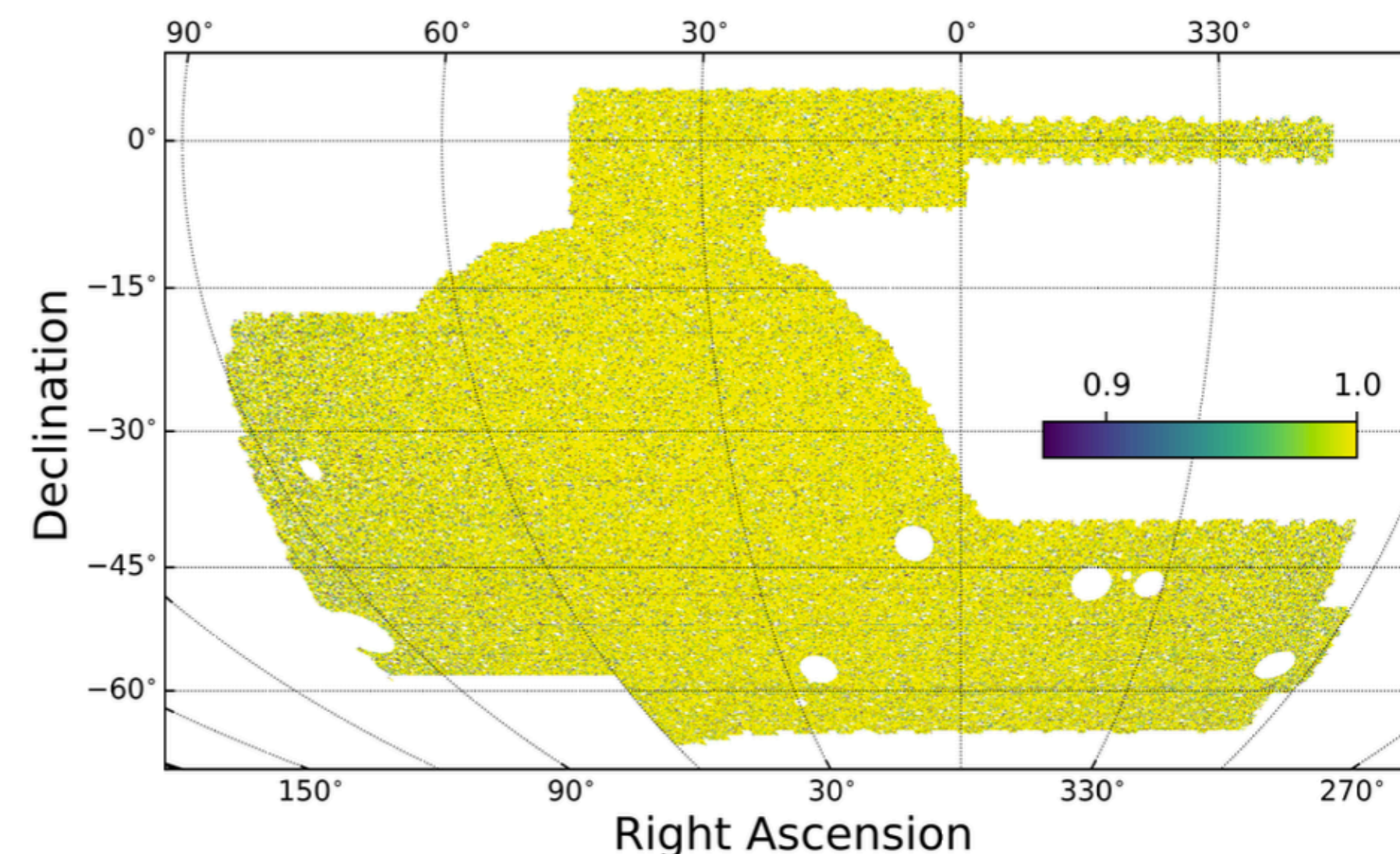


- Dark Energy Survey (DES) is an ongoing photometric survey.
- Use blanco 4-meter telescope at Cerro Tololo Inter-American Observatory in Chile
- Dark Energy Camera, Field of view: 3 sq deg, 570-megapixels CCD
- Y6 data collected from 2013 to 2019, last major official analyses



Y6 BAO sample overview

- Gold sample → BAO sample
- Area: 4273 sq. deg
- Redshift range: [0.6, 1.1] (Y3) → [0.6, 1.2]
- Number of gals: 15 937 556, x 2 wrt Y3



$$1.7 < i - z + 2(r - i),$$

$$17.5 < i < a + bz_{\text{ph}},$$

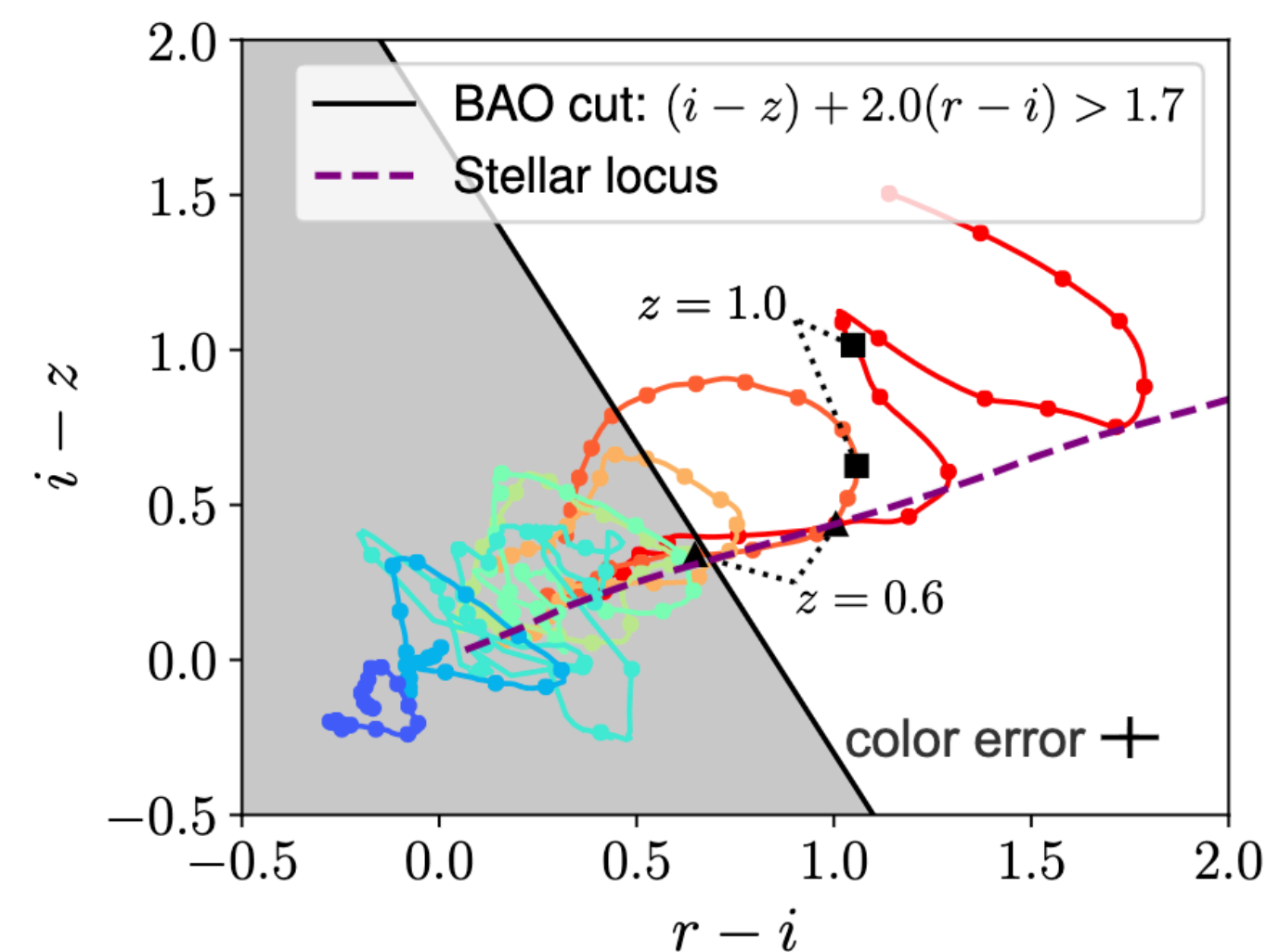
$$i < 22.5,$$

$$0.6 < z_{\text{ph}} < 1.2.$$

Red galaxy selection (high number density and bias, good photo-z)
reduced stellar continuations

Maximizing the BAO constraint,
(number density vs photo-z) $a=19.6$, $b=2.894$

J. Mena-Fernández +, in preparation



Crocce +, 1712.06211

Y6 sample properties

Y6

Bin	$\langle z_{\text{ph}} \rangle$	N_{gal}	σ_{68}
$0.6 < z_{\text{ph}} < 0.7$	0.654	2,854,542	0.0232
$0.7 < z_{\text{ph}} < 0.8$	0.752	3,266,097	0.0254
$0.8 < z_{\text{ph}} < 0.9$	0.844	3,898,672	0.0292
$0.9 < z_{\text{ph}} < 1.0$	0.929	3,404,744	0.0358
$1.0 < z_{\text{ph}} < 1.1$	1.013	1,752,169	0.0403
$1.1 < z_{\text{ph}} < 1.2$	1.107	761,332	0.0415

$$z_{\text{eff}} = 0.867, A = 4273.42 \text{deg}^2$$

Y3

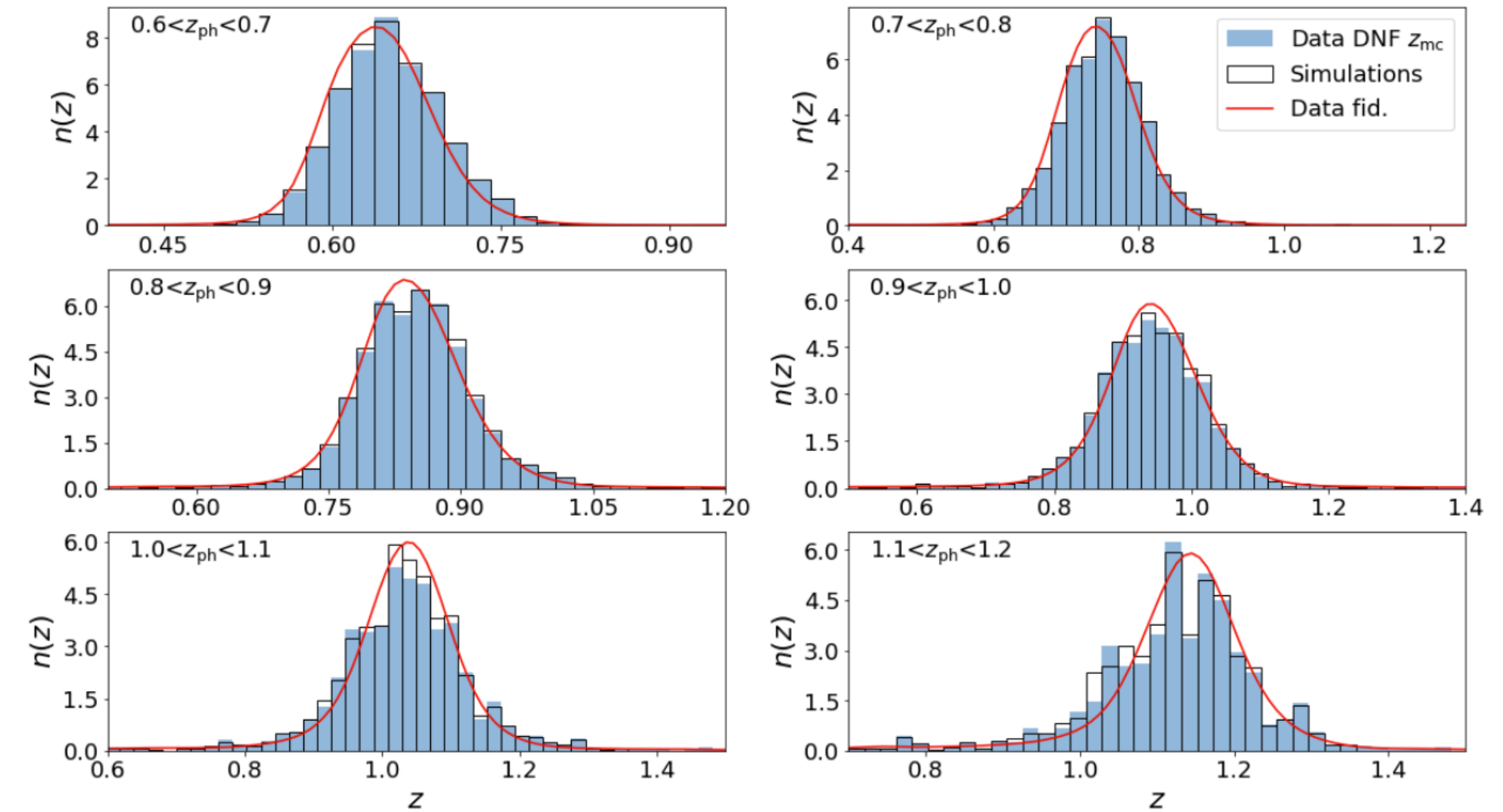
N_{gal}	$\sigma_{68} (*)$
1,478,178	0.0246
1,632,805	0.0279
1,727,646	0.0298
1,315,604	0.0363
877,760	0.0455

$$z_{\text{eff}} = 0.835, A = 4108.47 \text{deg}^2$$

- Double in sample size, better photo-z and one more redshift bin

Photo-z

- Photo-z is derived from DNF Z_MEAN, trained using grizY on a large of set spec-z data to establish the relation between magnitudes and true redshift
- Perform fitting in the color-magnitude space neighbor fitting to predict the redshift
- Z_MC (proxy for true-z distribution) is used in constructing ICE-COLA mock

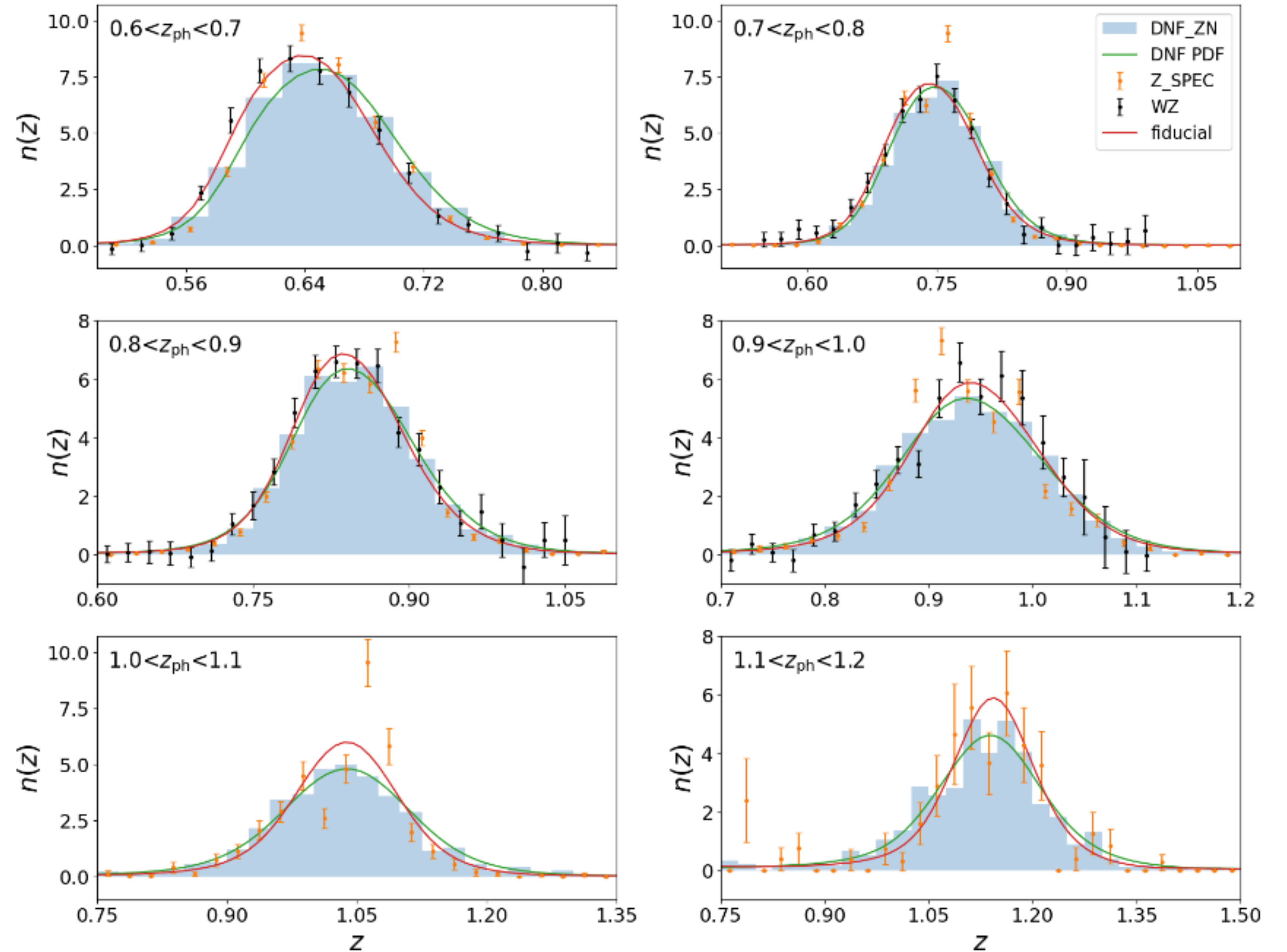
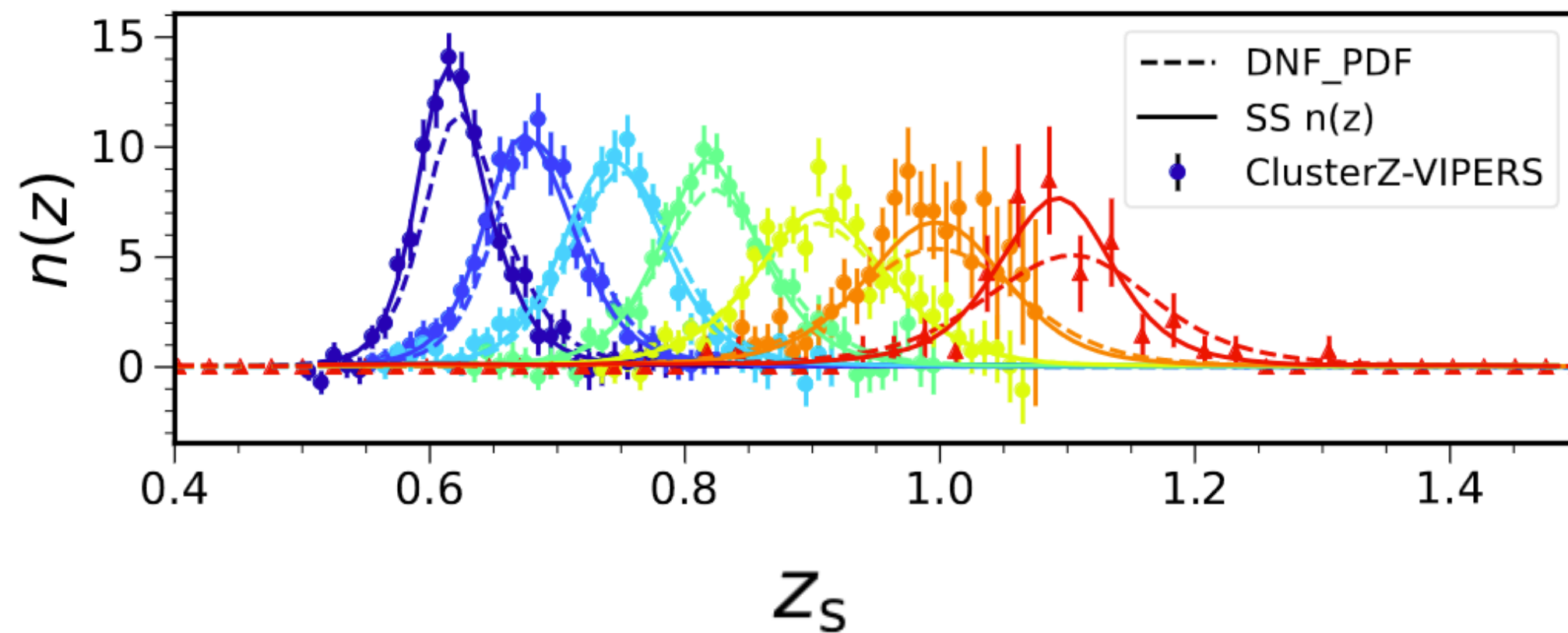


Bin	N_{gal}	σ_{68}
$0.6 < z_{\text{ph}} < 0.7$	2,854,542	0.0232
$0.7 < z_{\text{ph}} < 0.8$	3,266,097	0.0254
$0.8 < z_{\text{ph}} < 0.9$	3,898,672	0.0292
$0.9 < z_{\text{ph}} < 1.0$	3,404,744	0.0358
$1.0 < z_{\text{ph}} < 1.1$	1,752,169	0.0403
$1.1 < z_{\text{ph}} < 1.2$	761,332	0.0415

$$\sigma_{68} \approx \frac{z_p - z_s}{1 + z_s}$$

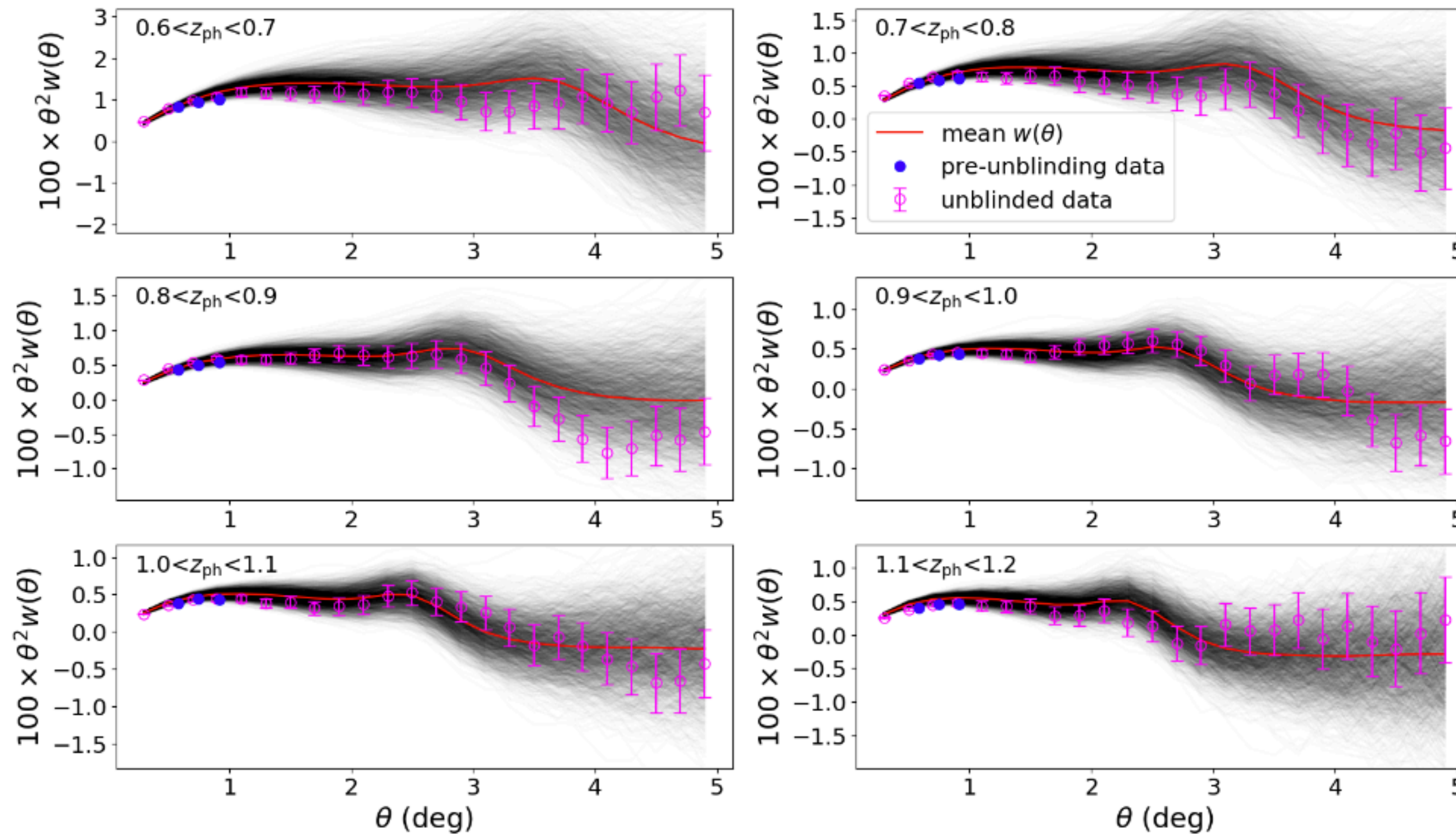
True-z distribution calibration

- True-z distribution for modeling is based on DNF PDF (green)
- Corrected by Shift & Stretched (Red) using Clustering-z ($z < 1$, Black) and VIPERS spec-z ($z > 1$, Orange)

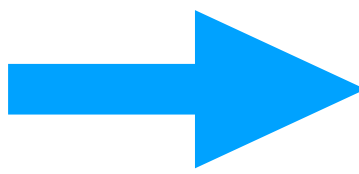


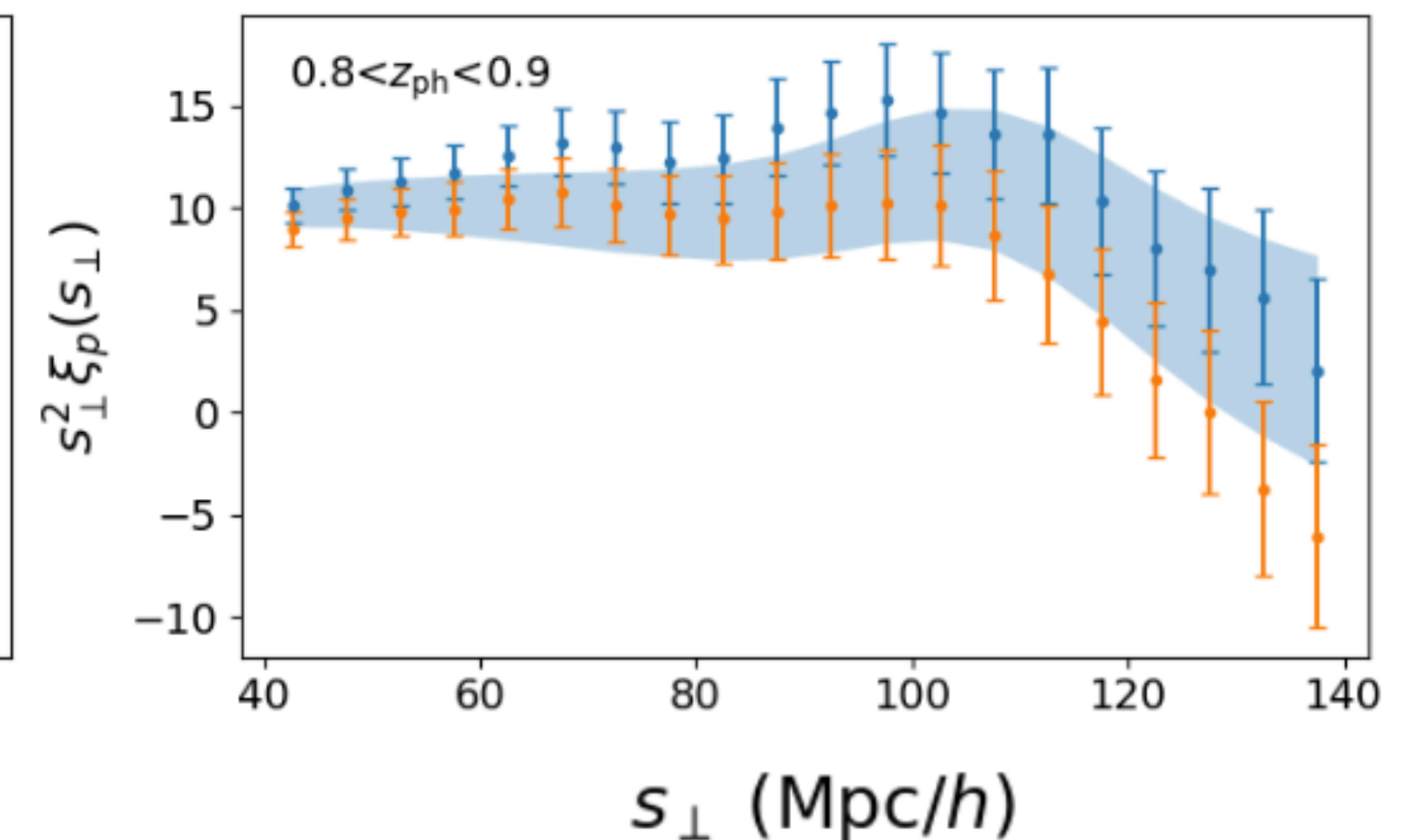
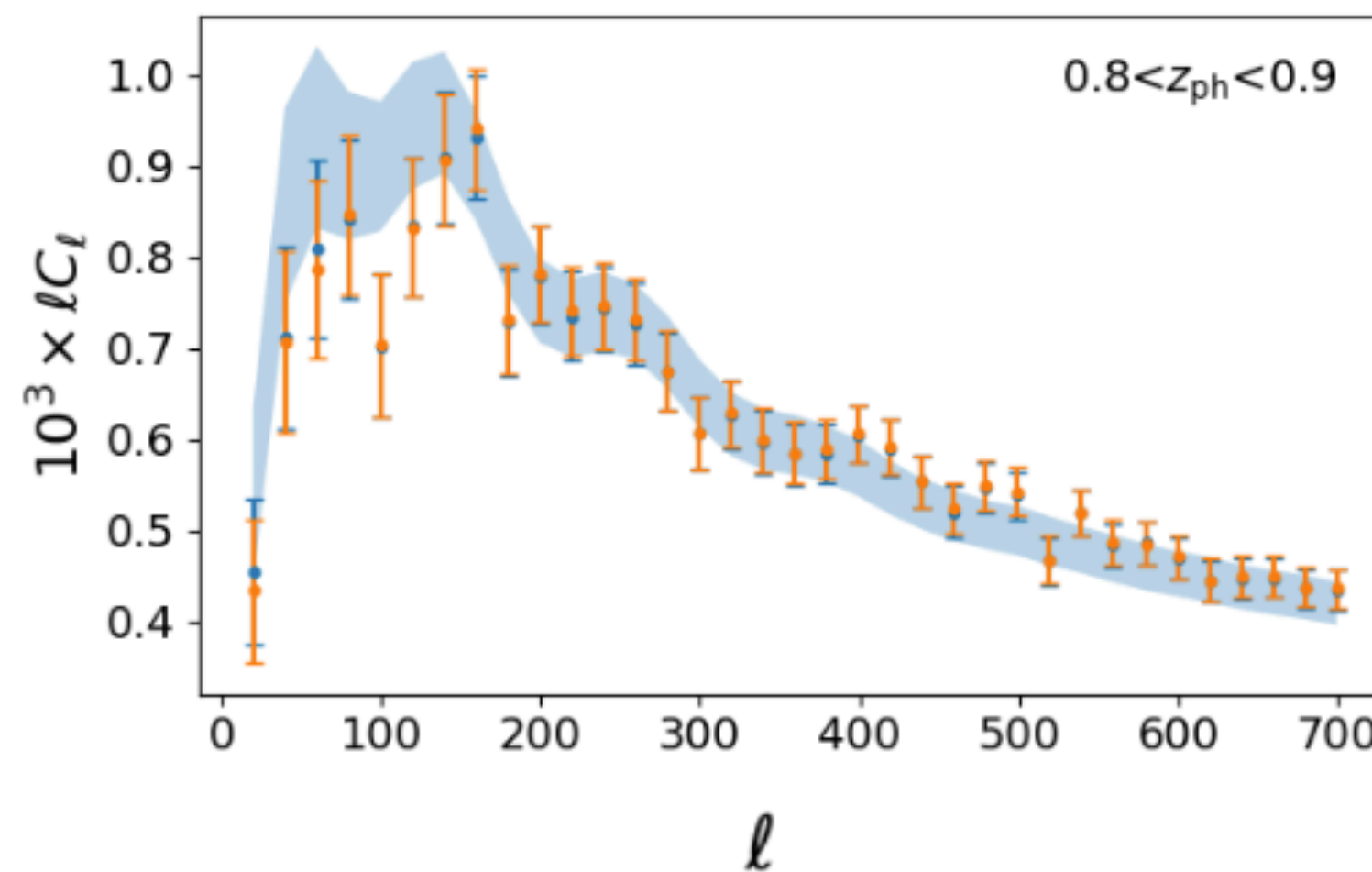
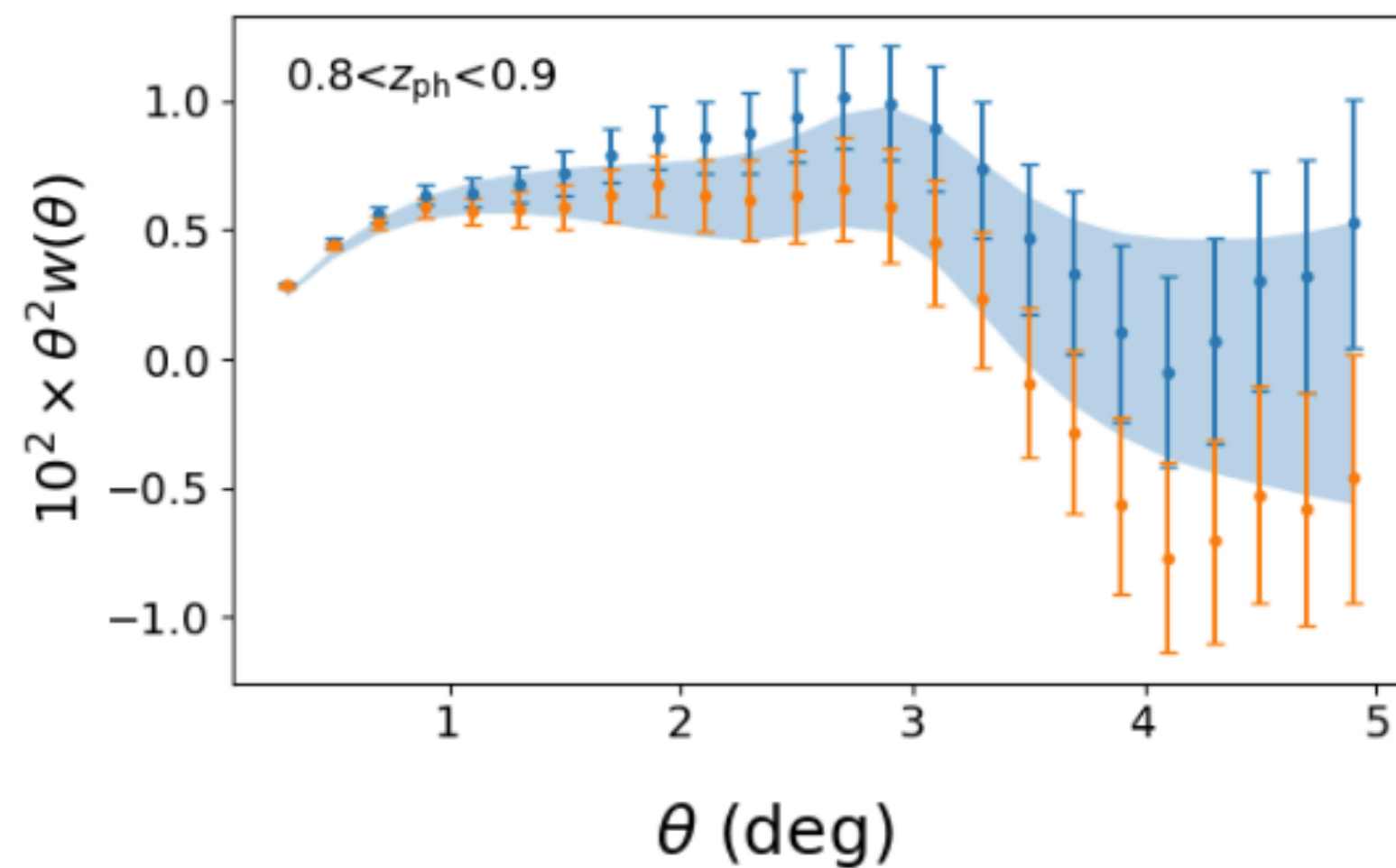
ICE-COLA mock catalog

- ICE-COLA mocks are used for pipeline testing
- 1952 mocks, match to Y6 properties



Three clustering statistics

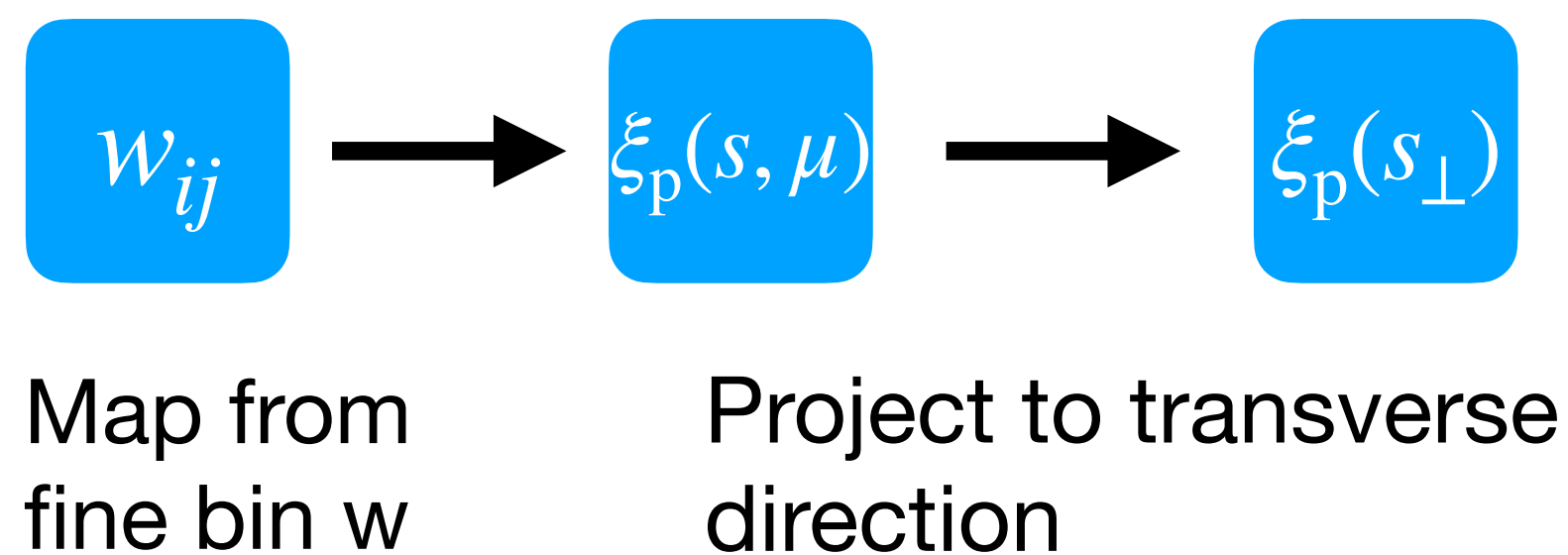
- Angular correlation function (ACF): w
 - Angular power spectrum (APS): C_ℓ  $\text{AVG} = w_1 \text{ACF} + w_2 \text{APS} + w_3 \text{PCF}$
 - Projective correlation function (PCF): ξ_p
- Consensus measurements**



Projected correlation function

- Treat photo-z data as per 3D data, derived the general cross correlation
- Reduce the photo-z smearing, project to the transverse direction.
- Include some radial direction info

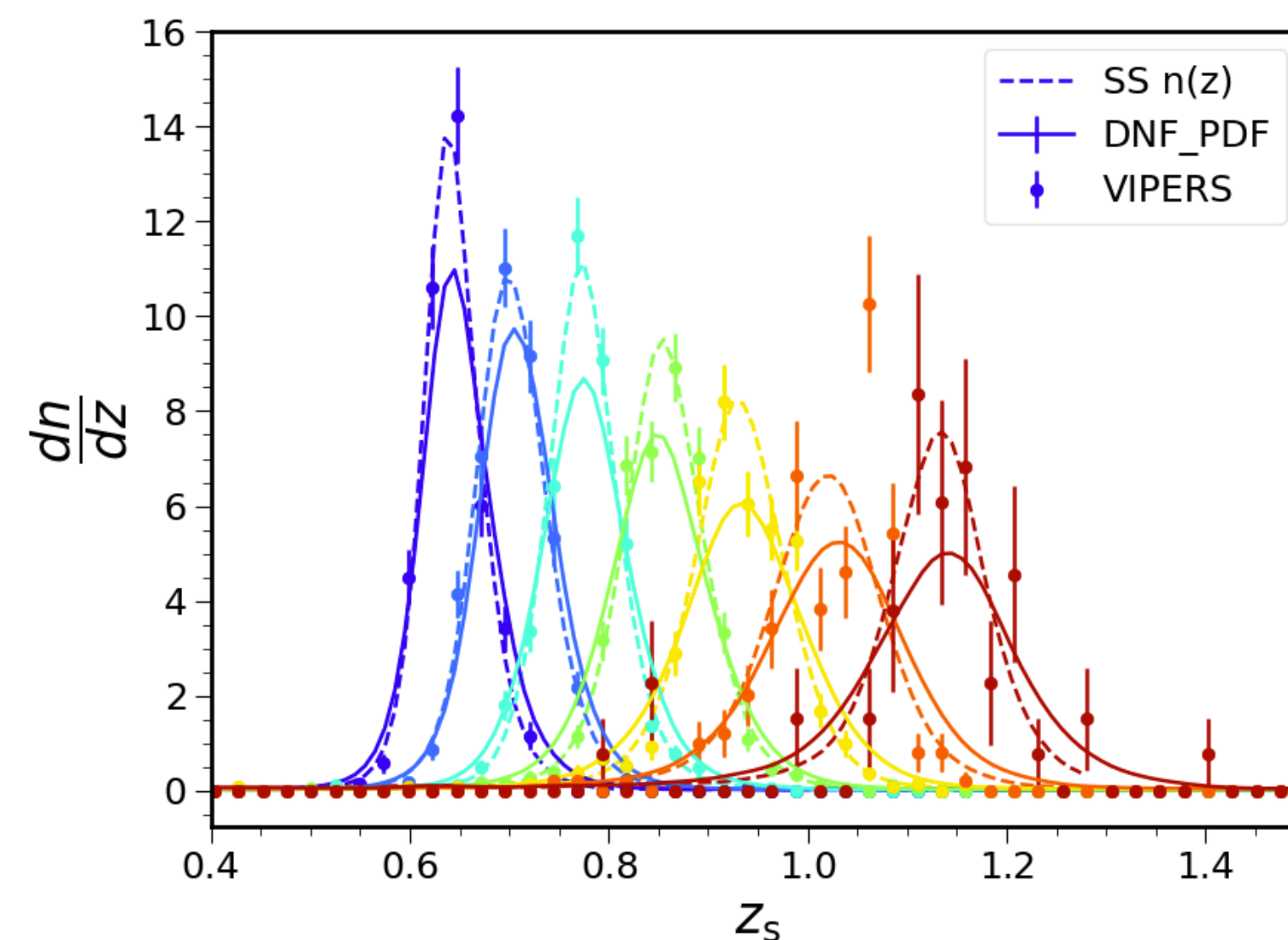
Template and covariance can be derived from the angular correlation results



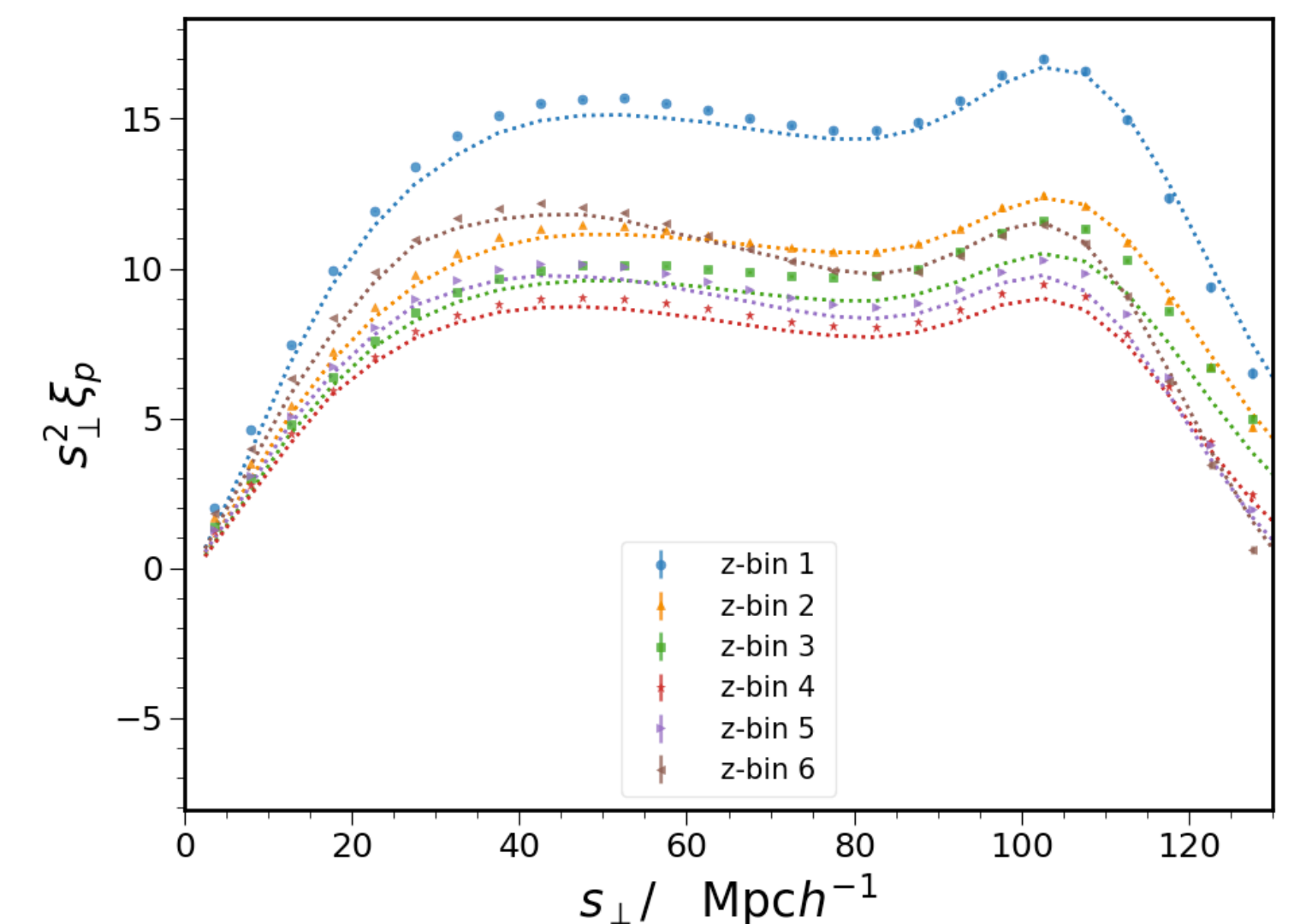
Ross +, 1705.05442

Chan +, 2110.13332

Fine bin photo-z,
22 adaptive bins



Six tomographic bins



Model fitting

$$P(k, \mu) = (b + \mu^2 f)^2 \left[(P_{\text{lin}} - P_{\text{nw}}) e^{-k^2 \Sigma^2} + P_{\text{nw}} \right]$$

$P(k)$ model



Clustering statistics template T

: w, C_ℓ, ξ_p

+

Nuisance para + $\alpha = \frac{D_M}{r_s} \frac{r_s}{D_M} \Big|_{\text{fid}}$

+

Covariance

+

Data measurement

χ^2
minimization



α or $\frac{D_M}{r_s}$

$$M(x) = BT_{\text{BAO}, \alpha}(x') + A(x)$$

Pre-unblinding tests on individual methods: **passed**

- Tests on the normality of the data while conforming to the blinding protocol
- Single failure of the test observed for ACF and APS, well within the expectation from mocks

ACF

Threshold (Fraction of mocks)	90 %		95 %		97 %		99 %		data	
	min	max	min	max	min	max	min	max	MICE	Planck
	$10^2(\alpha - \alpha_{\text{fiducial}})$									
Bins 23456	-1.33	1.43	-1.79	1.86	-2.10	2.17	-2.44	2.76	0.77	1.12
Bins 13456	-1.39	1.63	-1.83	1.99	-2.03	2.30	-2.80	3.13	1.02	1.39
Bins 12456	-1.37	1.51	-1.71	2.00	-2.03	2.35	-2.52	3.23	-0.25	-0.46
Bins 12356	-1.45	1.27	-1.81	1.57	-2.19	1.88	-2.80	2.76	-0.66	-0.31
Bins 12346	-1.21	1.11	-1.51	1.41	-1.79	1.72	-2.48	2.02	0.39	0.47
Bins 12345	-0.86	0.76	-1.07	0.96	-1.30	1.15	-1.63	1.65	-0.69	-0.84
Bins 456	-2.85	3.73	-3.42	4.85	-3.86	5.54	-5.00	7.90	3.17	3.28
Bins 123	-3.30	2.65	-4.27	3.45	-5.04	4.26	-6.80	5.56	-1.54	-1.59
Bins 1234	-1.83	1.67	-2.25	2.13	-2.55	2.35	-3.67	3.22	-0.38	-0.77
Template Cosmo	-0.33	0.48	-0.40	0.60	-0.44	0.68	-0.55	0.89	x	0.22
Covariance	-0.46	0.42	-0.58	0.54	-0.68	0.64	-0.83	0.82	x	-0.48
$n(z)$ z_{mc} -fid	-0.56	0.08	-0.60	0.14	-0.64	0.20	-0.72	0.31	x	-0.48
	$100(\sigma - \sigma_{\text{All Bins}})/\sigma_{\text{All Bins}}$									
Bins 23456	-2.47	25.15	-4.33	30.34	-6.09	35.42	-9.08	41.50	5.83	3.06
Bins 13456	-1.60	26.16	-3.55	31.21	-5.18	35.18	-8.95	45.61	18.45	13.97
Bins 12456	-2.00	26.22	-4.53	31.44	-5.84	36.80	-8.93	45.86	17.48	14.85
Bins 12356	-2.29	25.17	-4.09	30.79	-5.51	35.11	-9.35	41.35	8.74	4.37
Bins 12346	-1.39	19.89	-2.84	24.51	-4.07	27.92	-6.22	34.80	7.77	7.42
Bins 12345	-0.66	11.94	-1.45	14.87	-1.97	17.79	-3.56	22.50	0.49	-3.06
Bins 456	12.08	94.25	8.20	114.76	5.13	128.50	-1.76	166.46	65.05	56.33
Bins 123	10.14	80.86	5.92	95.62	3.02	109.42	-2.36	144.43	22.82	18.34
Bins 1234	1.37	35.50	-0.99	42.58	-1.84	45.70	-4.23	55.74	7.77	4.80

APS

Threshold (Fraction of mocks)	0.9		0.95		0.97		0.99		data	
	min	max	min	max	min	max	min	max	MICE	Planck
	$10^2(\alpha - \alpha_{\text{fiducial}})$									
Bins 23456	-1.18	1.45	-1.59	1.85	-2.01	2.12	-2.99	3.19	0.24	0.54
Bins 13456	-1.46	1.55	-1.88	2.26	-2.24	2.76	-3.54	3.60	1.44	1.76
Bins 12456	-1.32	1.48	-1.82	2.07	-2.14	2.71	-2.75	4.22	-0.22	-0.29
Bins 12356	-1.55	1.28	-2.05	1.79	-2.63	2.10	-4.36	3.08	-0.21	-0.22
Bins 12346	-1.48	1.43	-2.01	1.91	-2.67	2.49	-3.96	3.31	1.22	0.65
Bins 12345	-1.59	1.45	-2.10	2.00	-2.67	2.42	-3.95	3.60	-1.50	-1.39
Bins 456	-2.68	3.75	-3.25	4.91	-4.08	5.56	-5.96	8.06	2.31	3.25
Bins 123	-4.58	3.44	-6.16	4.46	-7.80	5.49	-14.48	7.00	-1.32	-1.83
Bins 1234	-2.78	2.47	-3.87	3.37	-4.58	4.29	-6.38	6.17	-0.79	-1.13
Template Cosmo	-0.59	0.62	-0.72	0.83	-0.89	0.99	-1.20	1.60	x	-0.49
Covariance	-0.57	0.62	-0.75	0.79	-0.91	0.91	-1.30	1.38	x	-0.09
$n(z)$	-0.35	0.61	-0.47	0.69	-0.55	0.75	-0.78	0.89	x	-0.20
	$100(\sigma - \sigma_{\text{All Bins}})/\sigma_{\text{All Bins}}$									
Bins 23456	-5.53	28.15	-7.91	34.95	-10.77	44.11	-16.41	61.14	-1.43	0.72
Bins 13456	-5.06	33.65	-8.46	40.63	-11.21	47.60	-18.61	78.34	13.66	18.11
Bins 12456	-5.09	29.11	-8.63	37.93	-10.67	45.63	-15.98	54.38	24.22	21.10
Bins 12356	-6.17	33.22	-9.39	45.05	-12.03	49.74	-22.23	62.51	8.37	10.48
Bins 12346	-5.67	31.74	-9.73	41.92	-12.71	47.79	-19.20	73.87	13.52	12.11
Bins 12345	-4.89	30.92	-7.90	42.62	-10.77	52.16	-18.77	75.55	-6.10	-7.55
Bins 456	-0.98	97.42	-7.16	130.80	-12.08	155.71	-18.40	203.90	46.17	53.50
Bins 123	1.81	126.95	-3.37	160.80	-7.36	189.98	-17.54	257.44	24.42	16.35
Bins 1234	-3.89	70.89	-7.83	86.84	-12.27	104.47	-22.21	156.87	7.86	1.54

PCF

Threshold (Fraction of mocks)	0.9		0.95		0.97		0.99		data	
	min	max	min	max	min	max	min	max	MICE	Planck
	$10^2(\alpha - \alpha_{\text{fiducial}})$									
Bins 23456	-1.72	1.48	-2.12	1.92	-2.32	2.12	-2.96	2.77	0.88	0.96
Bins 13456	-1.48	1.32	-1.86	1.72	-2.12	1.92	-2.65	2.63	-0.32	-0.20
Bins 12456	-1.28	1.28	-1.64	1.70	-2.00	2.04	-2.53	2.89	0.16	0.24
Bins 12356	-1.16	1.16	-1.46	1.60	-1.68	1.92	-2.57	2.37	-0.48	-0.56
Bins 12346	-0.76	0.96	-1.00	1.20	-1.16	1.52	-1.60	2.00	0.20	0.24
Bins 12345	-0.44	0.52	-0.60	0.64	-0.68	0.72	-0.85	0.88	-0.24	-0.28
Bins 456	-3.76	3.24	-4.85	4.28	-5.40	4.88	-6.59	6.47	2.28	2.32
Bins 123	-1.92	2.44	-2.48	3.12	-2.96	3.52	-4.35	4.36	-1.04	-1.44
Bins 1234	-1.00	1.32	-1.28	1.66	-1.52	1.88	-1.94	2.48	-0.08	-0.12
Template Cosmo	-0.80	0.92	-1.01	1.12	-1.13	1.20	-1.49	1.49	x	0.13
Covariance	-0.40	0.48	-0.48	0.60	-0.56	0.68	-0.73	0.84	x	-0.12
$n(z)$ z_{mc} -fid	-0.40	-0.08	-0.44	-0.04	-0.44	0.00	-0.49	0.04	x	-0.27
	$100(\sigma - \sigma_{\text{All Bins}})/\sigma_{\text{All Bins}}$									
Bins 23456	-1.12	32.11	-3.30	40.01	-4.62	45.33	-6.56	55.20	3.23	4.97
Bins 13456	-1.12	27.14	-2.80	32.06	-3.99	37.51	-6.23	47.73	18.28	16.57
Bins 12456	-1.97	23.91	-3.41	28.78	-4.54	33.69	-6.91	40.64	10.75	6.95
Bins 12356	-1.02	22.99	-2.61	27.89	-3.21	33.89	-5.85	40.96	6.45	7.95
Bins 12346	0.00	15.35	-1.49	18.40	-2.20	20.89	-3.80	26.56	7.53	9.60
Bins 12345	0.00	7.00	-1.14	8.93	-1.34	10.48	-2.12	12.19	2.15	1.32
Bins 456	18.11	124.49	14.14	150.21	10.89	169.93	5.18	222.60	67.74	50.00
Bins 123	6.09	58.36	4.35	69.50	2.92	75.66	-1.03	94.05	22.58	27.15
Bins 1234	8.46	19.08	0.00	26.12	-0.97	29.96	-2.36	37.06	8.60	11.59

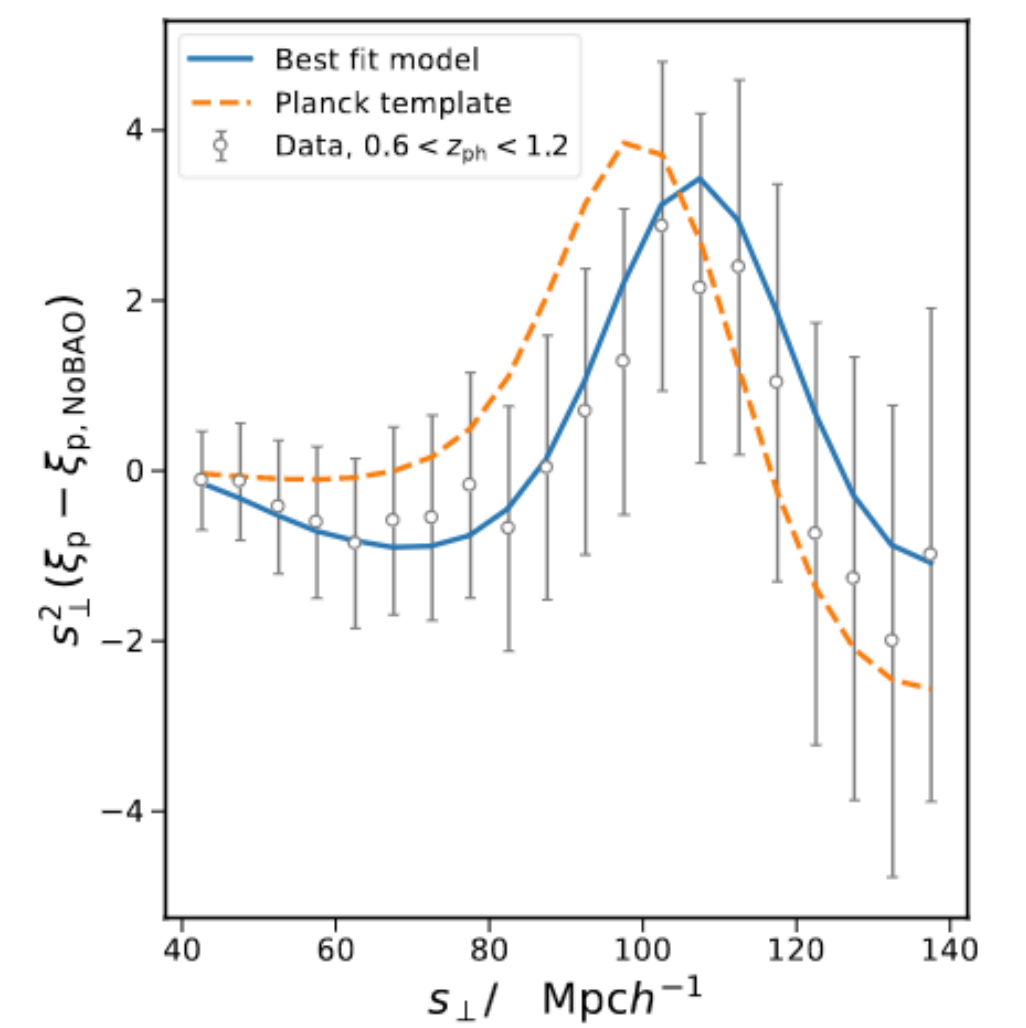
Y6 BAO measurements

- The combined consensus BAO measurement

$$\alpha = 0.9571 \pm 0.0196 \text{ [stat.],}$$

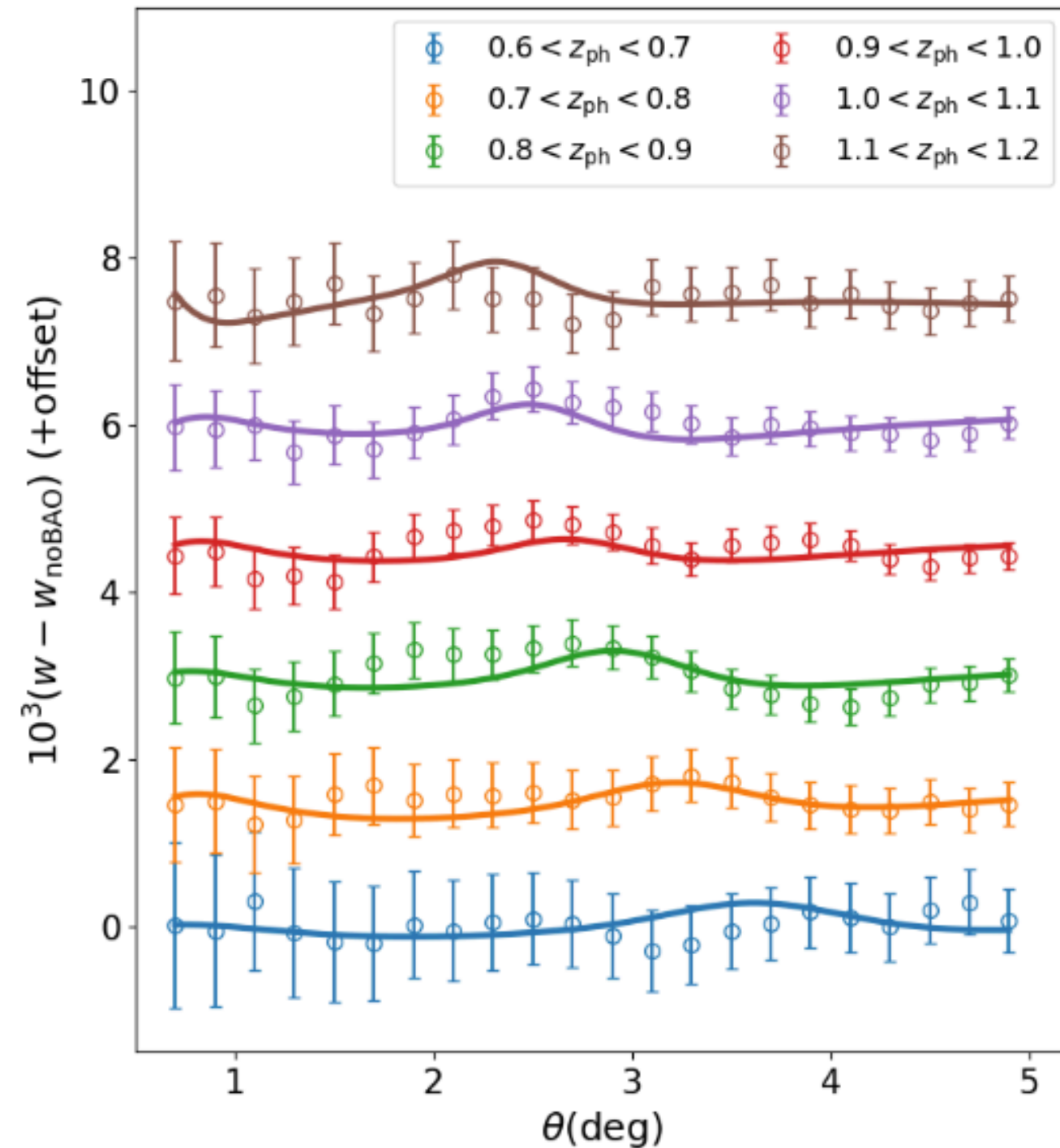
$$\pm 0.0041 \text{ [sys.],}$$

$$\alpha = 0.9571 \pm 0.0201 \text{ [tot.]}$$



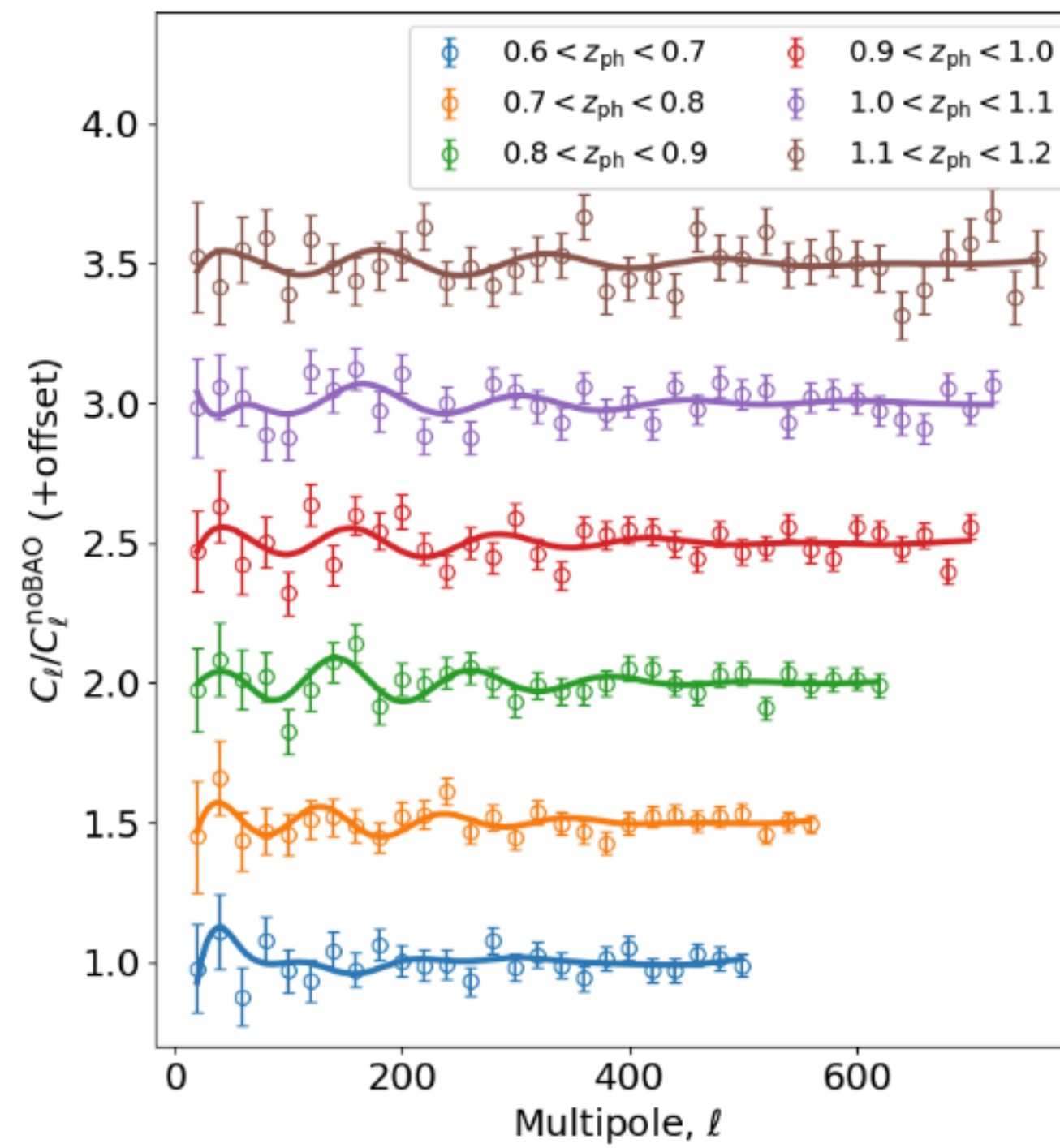
ACF, w

$$\alpha = 0.9517 \pm 0.0227$$



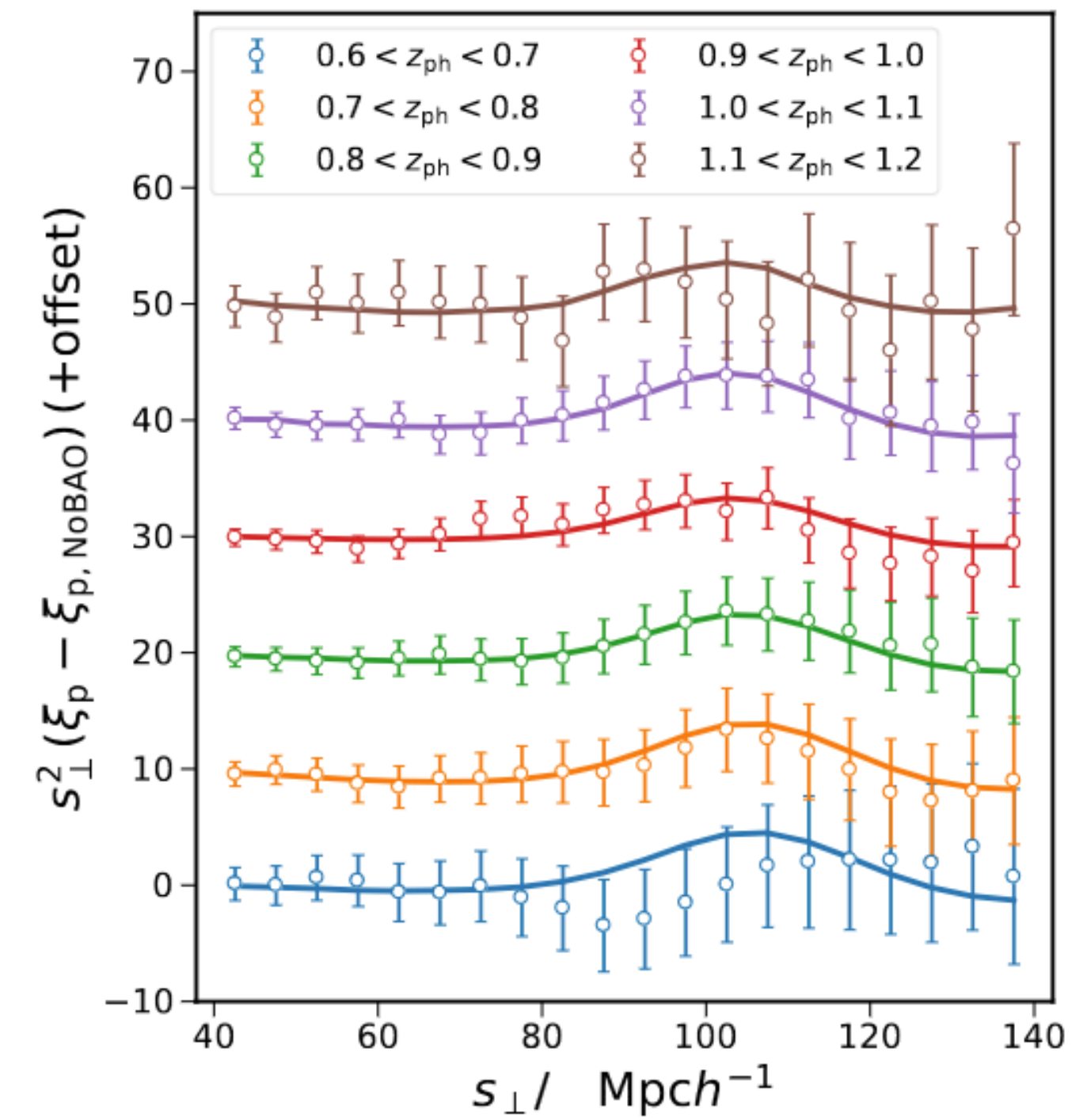
APS, C_ℓ

$$\alpha = 0.9617 \pm 0.0224$$



PCF, ξ_p

$$\alpha = 0.9553 \pm 0.0201$$

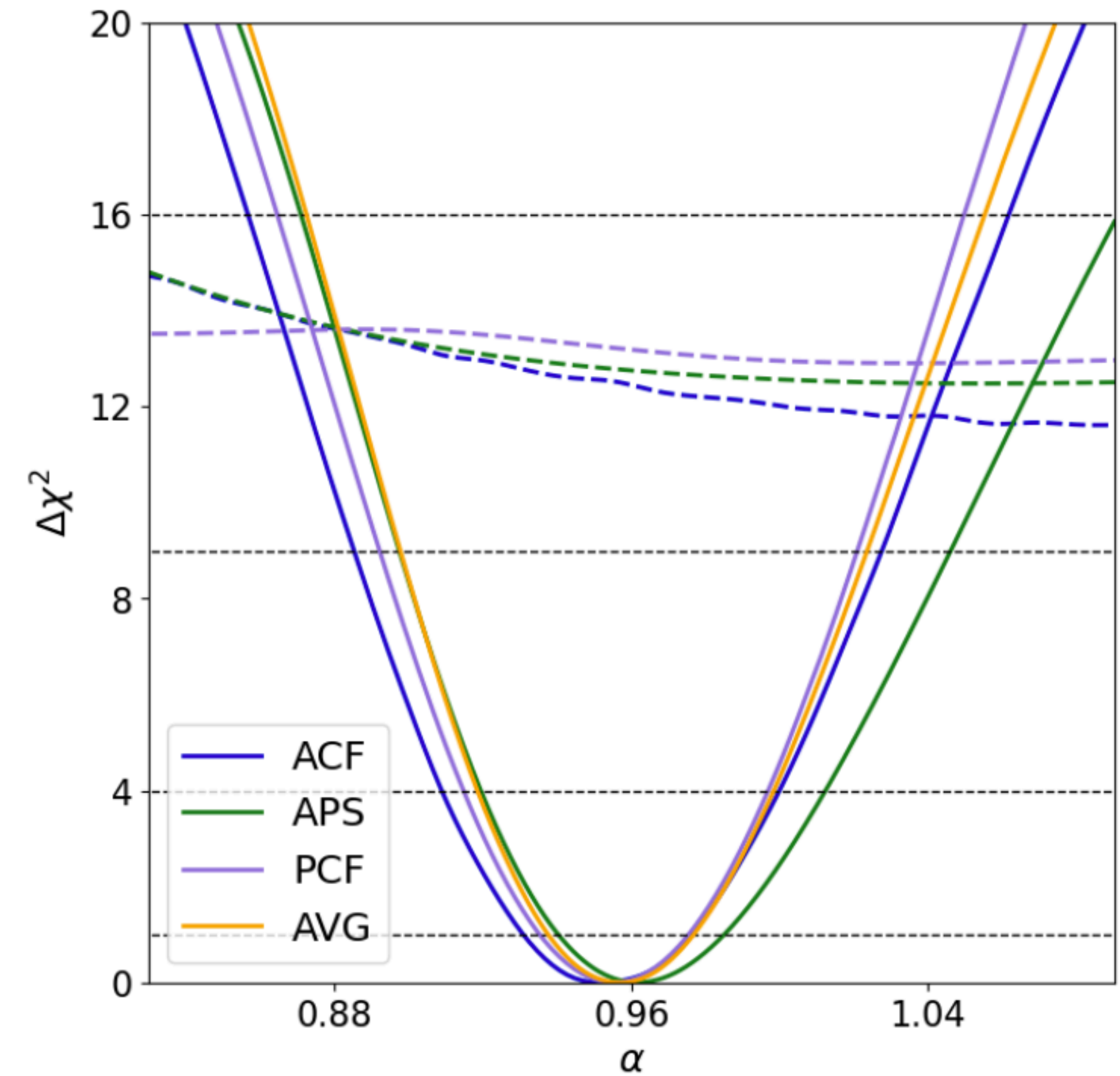


Y6 BAO measurements

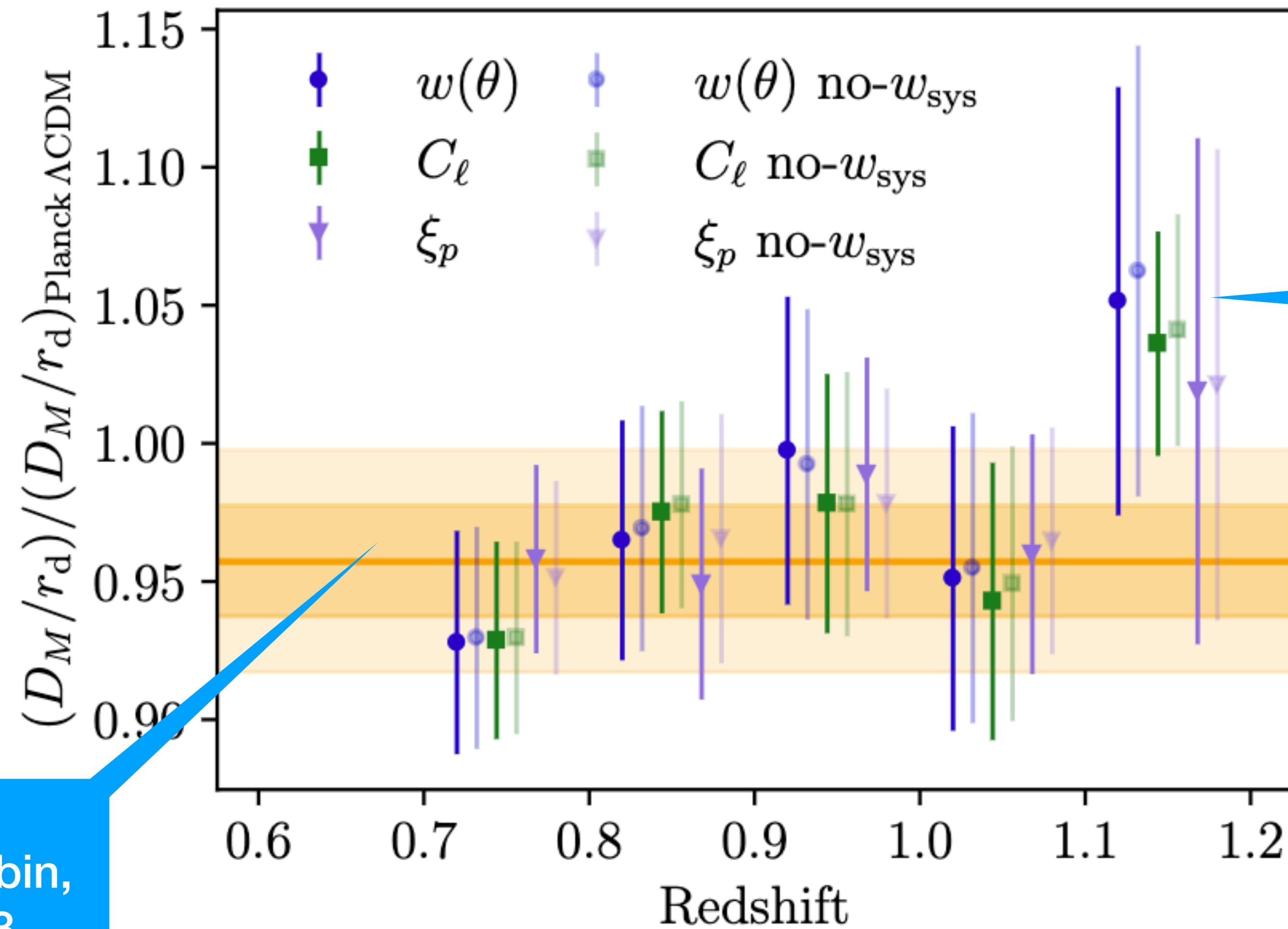
- 3.5 σ detection of BAO

$$\alpha = 0.9571 \pm 0.0201 \text{ [tot.]}$$

$$D_M(z = 0.87)/r_d = 19.79 \pm 0.42 \text{ [tot.]}$$



Individual bin measurements



No detection in first bin,
same in Y1 and Y3

Highest redshift bin
show the largest
deviation from the low
bins, but its
contribution to final
constraint is weak

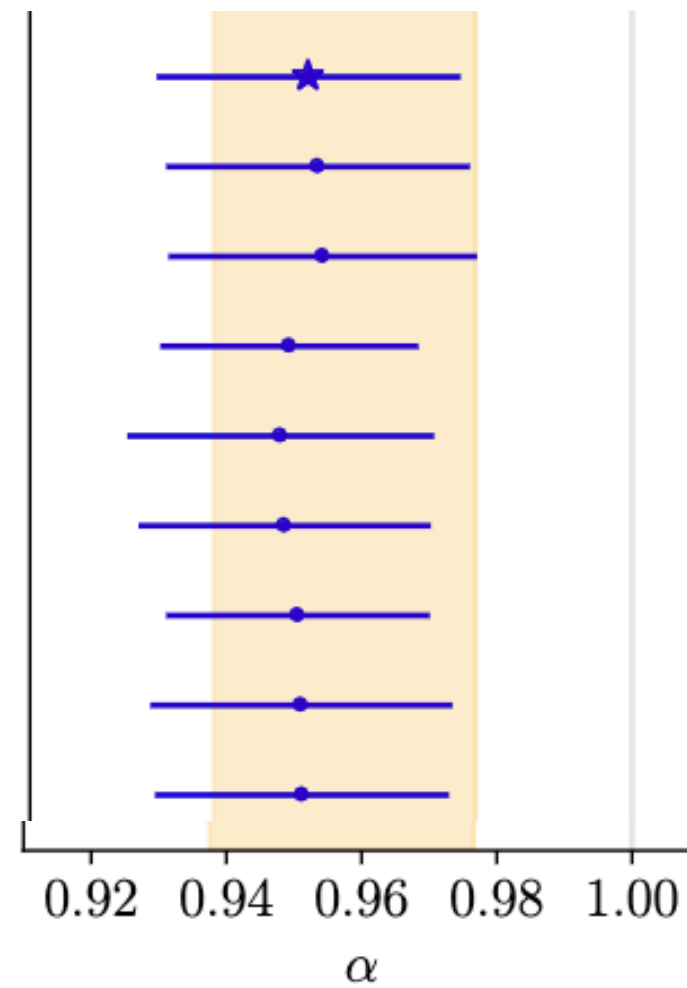
Robustness tests

- The change in the best fit α is within 1σ

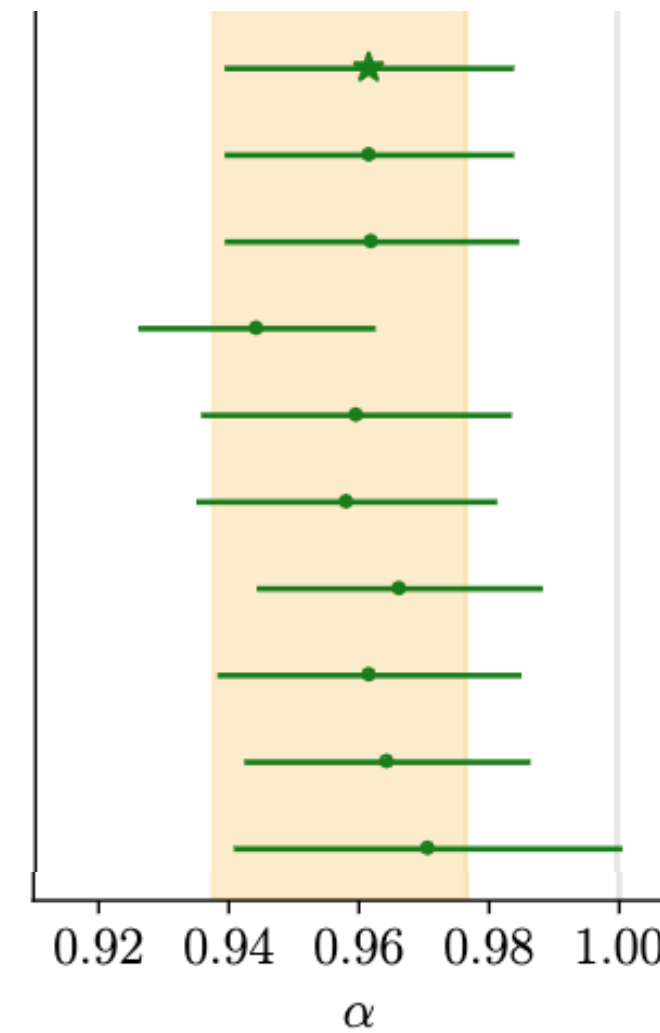
$$\begin{array}{l} \mathbf{w}(\theta) + \mathbf{C}_\ell + \xi_p \\ w(\theta) + C_\ell + \xi_p \text{ (} w_{\text{sys}} \text{ w/o } Y \text{)} \end{array}$$



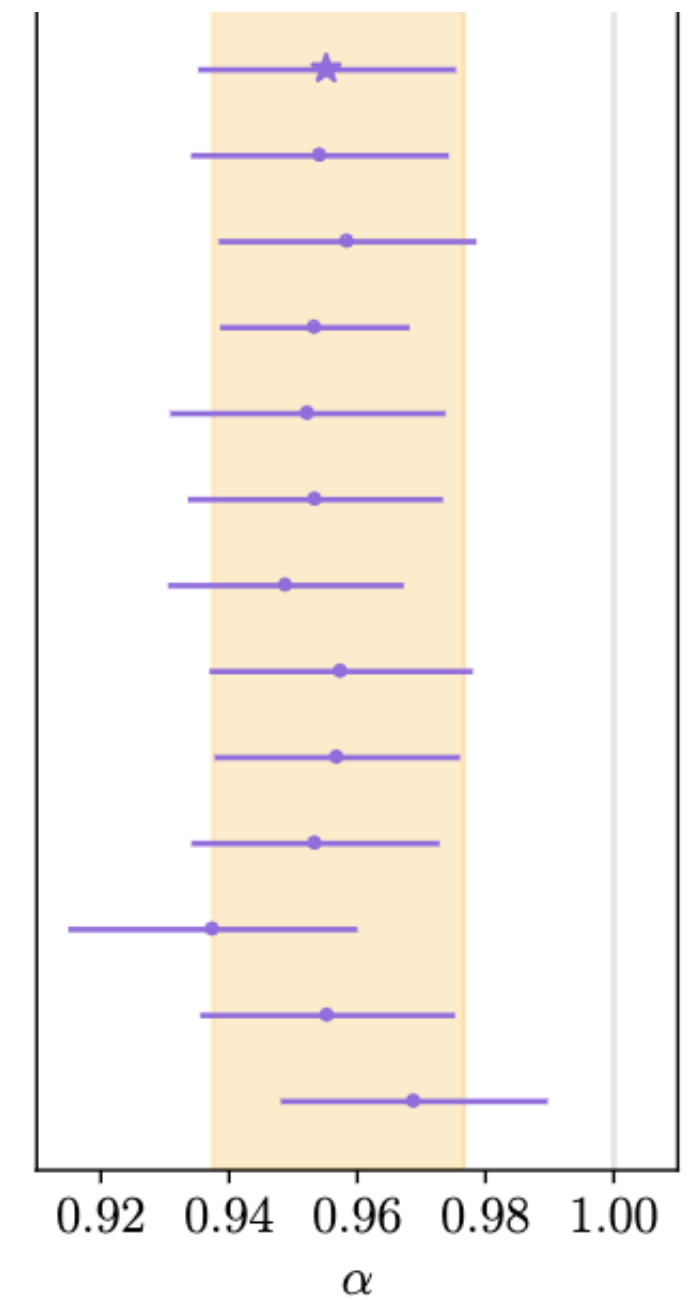
$\mathbf{w}(\theta)$
 $w(\theta) \text{ } w_{\text{sys}} \text{ w/o } Y$
 $w(\theta) \text{ no-}w_{\text{sys}}$
 $w(\theta) \text{ mocks-Cov}$
 $w(\theta) \text{ DNF } n(z_{\text{nn}})$
 $w(\theta) \text{ Vipers } n(z)$
 $w(\theta) \text{ MICE } \times 0.9616$
 $w(\theta) \theta_{\text{min}} = 1^\circ$
 $w(\theta) \Delta\theta = 0.1^\circ$



\mathbf{C}_ℓ
 $C_\ell \text{ } w_{\text{sys}} \text{ w/o } Y$
 $C_\ell \text{ no-}w_{\text{sys}}$
 $C_\ell \text{ mocks-Cov}$
 $C_\ell \text{ DNF } n(z_{\text{nn}})$
 $C_\ell \text{ Vipers } n(z_{\text{spec}})$
 $C_\ell \text{ MICE } \times 0.9616$
 $C_\ell \ell_{\text{max}}$
 $C_\ell \Delta\ell = 10$
 $C_\ell \Delta\ell = 30$

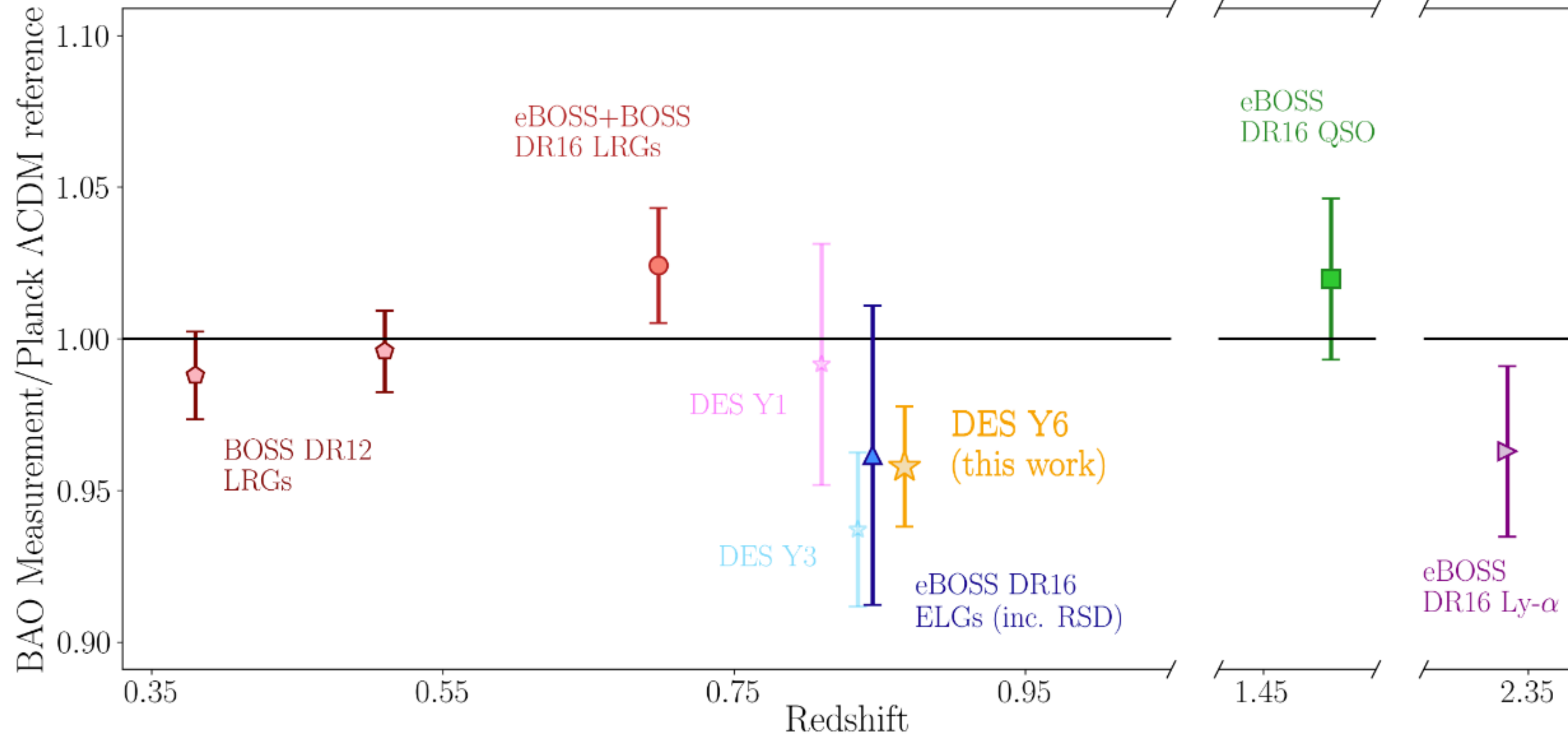


ξ_p
 $\xi_p \text{ } w_{\text{sys}} \text{ w/o } Y$
 $\xi_p \text{ no-}w_{\text{sys}}$
 $\xi_p \text{ mock-Cov}$
 $\xi_p \text{ DNF } n(z_{\text{nn}})$
 $\xi_p \text{ Vipers } n(z_{\text{spec}})$
 $\xi_p \text{ MICE } \times 0.9616$
 $\xi_p \text{ } s \in [70, 130]h^{-1}\text{Mpc}$
 $\xi_p \Delta s = 10h^{-1}\text{Mpc}$
 $\xi_p \Delta s = 2h^{-1}\text{Mpc}$
 $\xi_p N_z = 1$
 $\xi_p N_z = 3$
 $\xi_p N_z = 1, 0.7 < z < 1.2$



Y6 BAO measurement

- Y6 is the most precise photometric BAO measurement
- The most precise transverse BAO measurement at $z \sim 0.8$

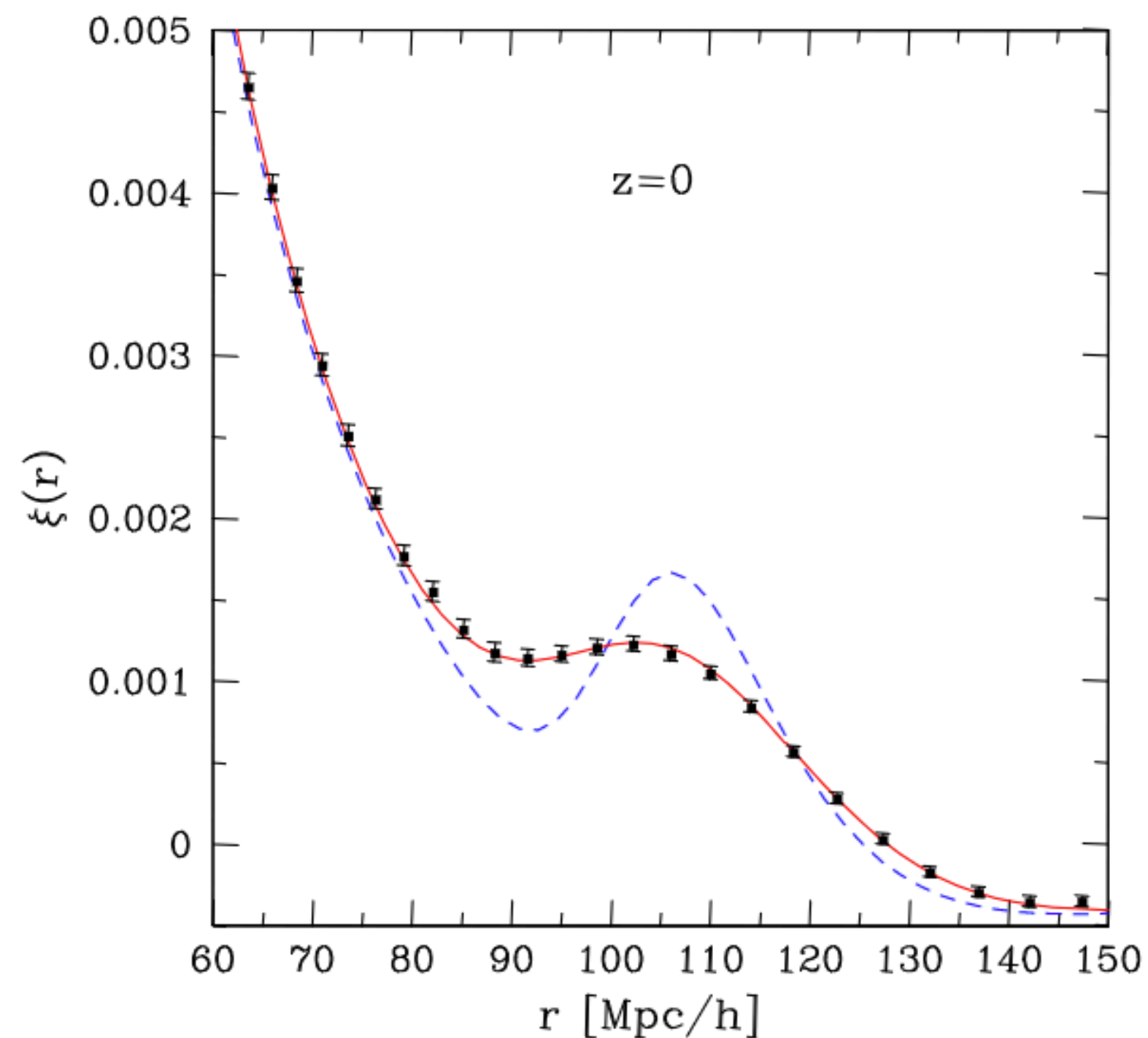


Photometric BAO reconstruction

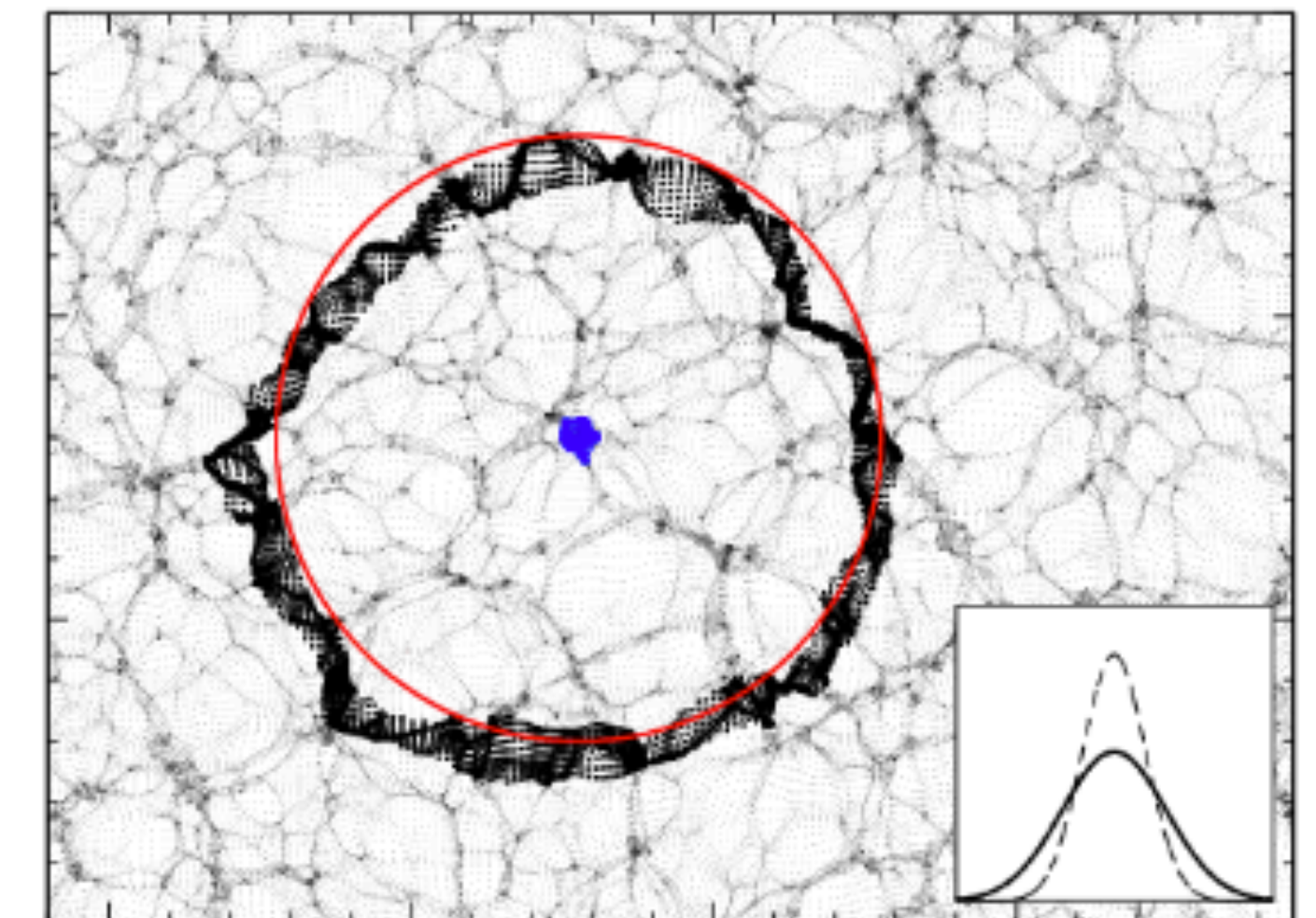
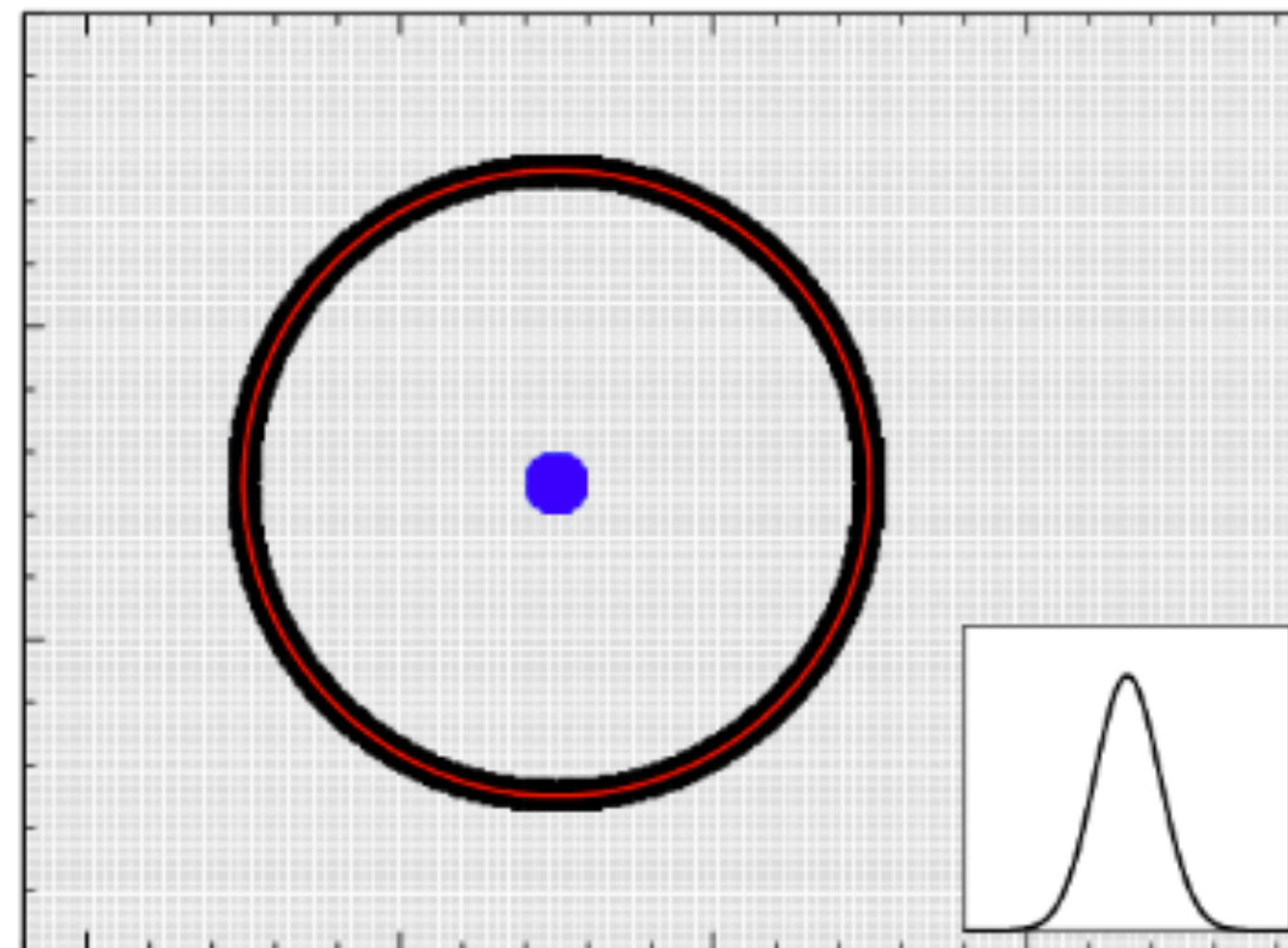
KCC + , 2311.12611

Damping of the BAO

- Large scale bulk flow causes the BAO feature to be damped over time



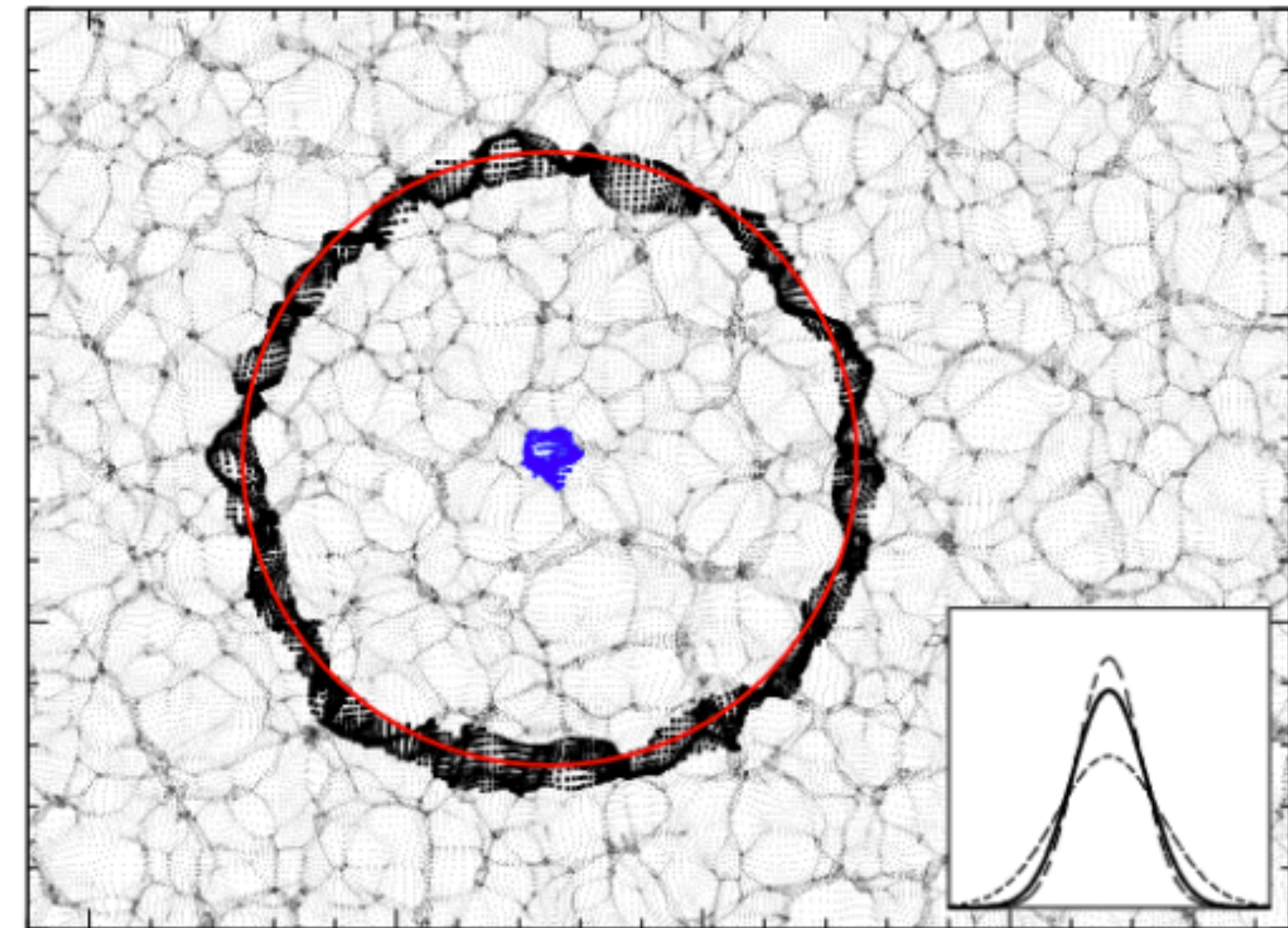
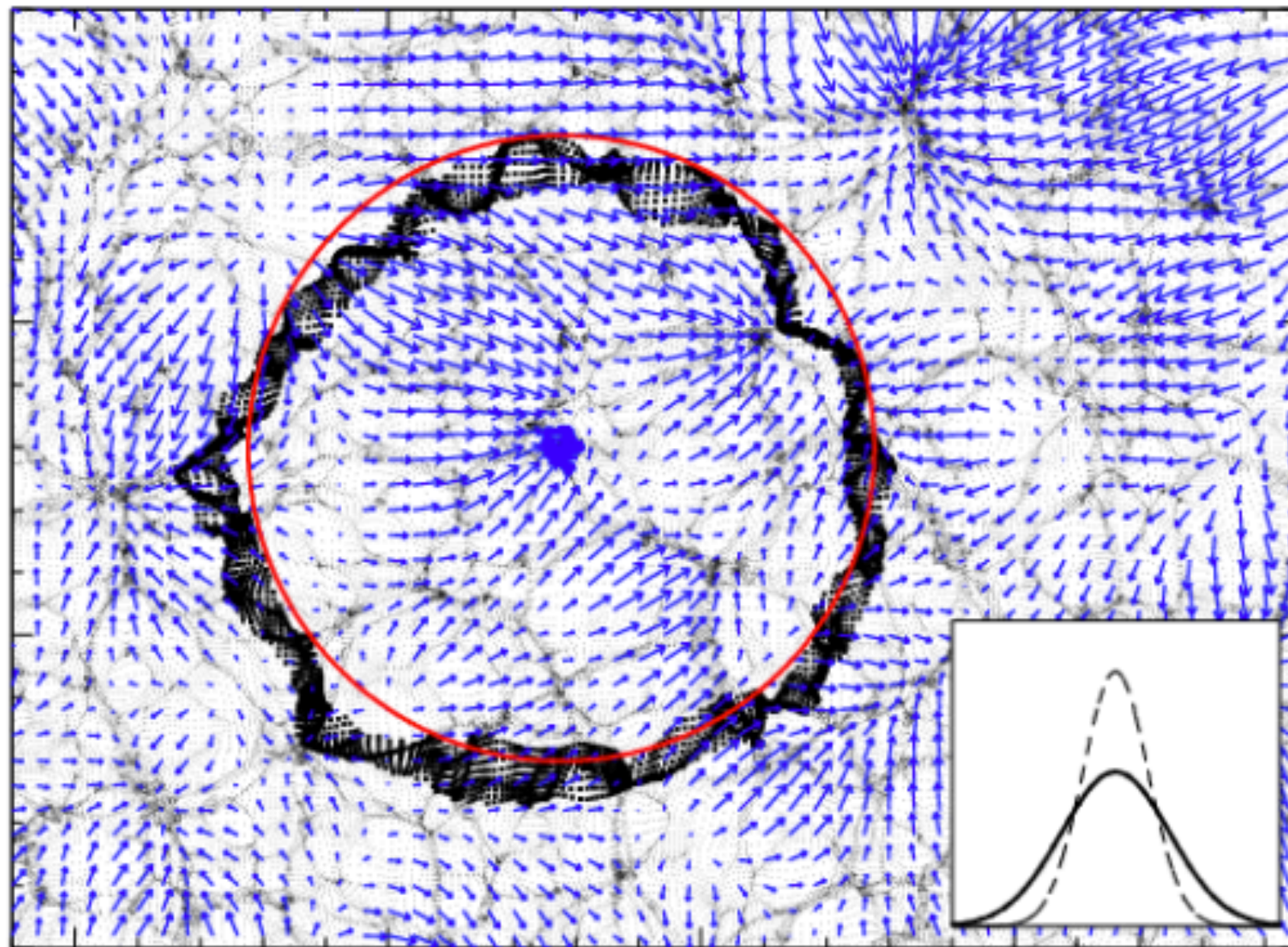
Crocce & Scoccimarro 2007



Padmanabhan +, 2012

BAO reconstruction

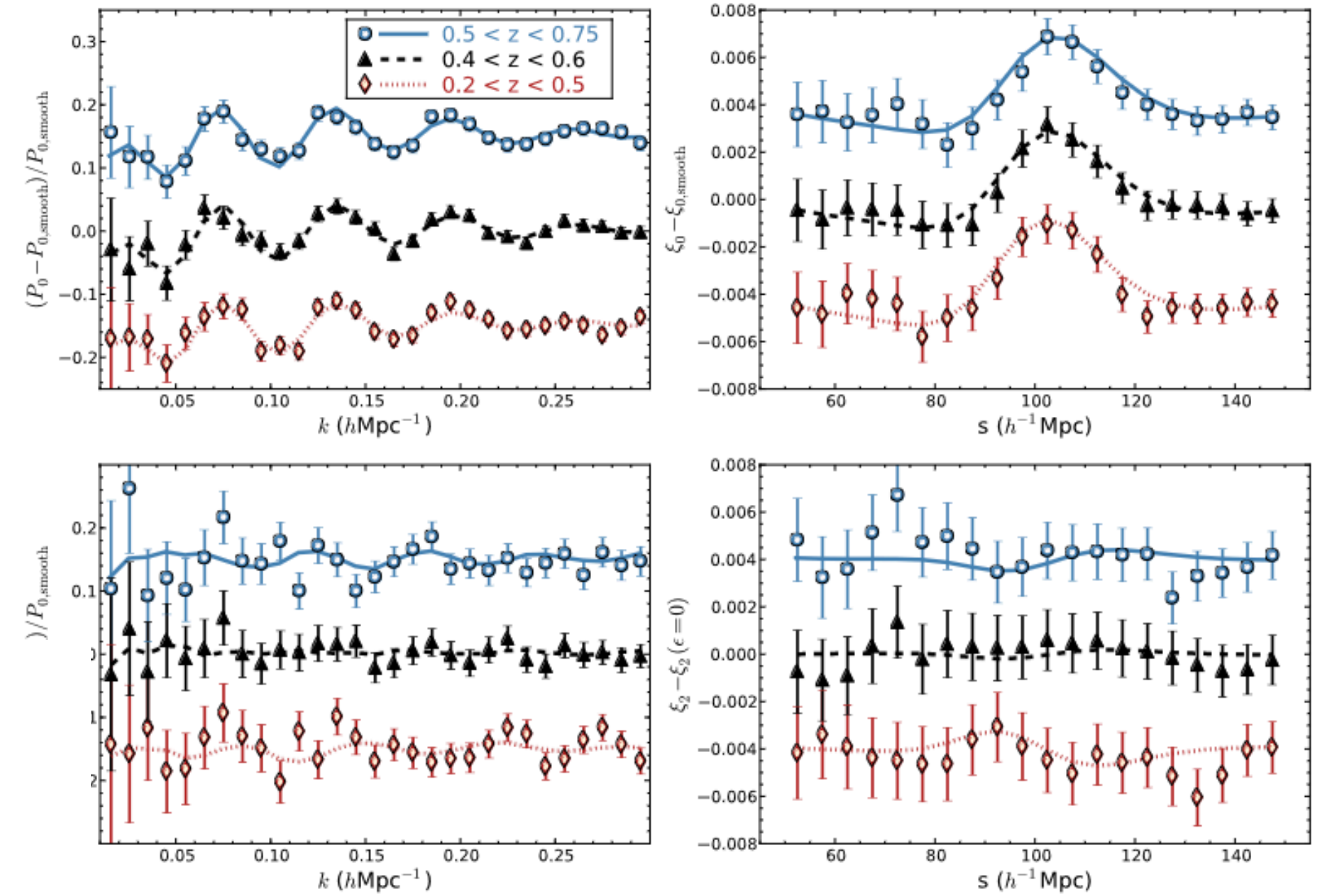
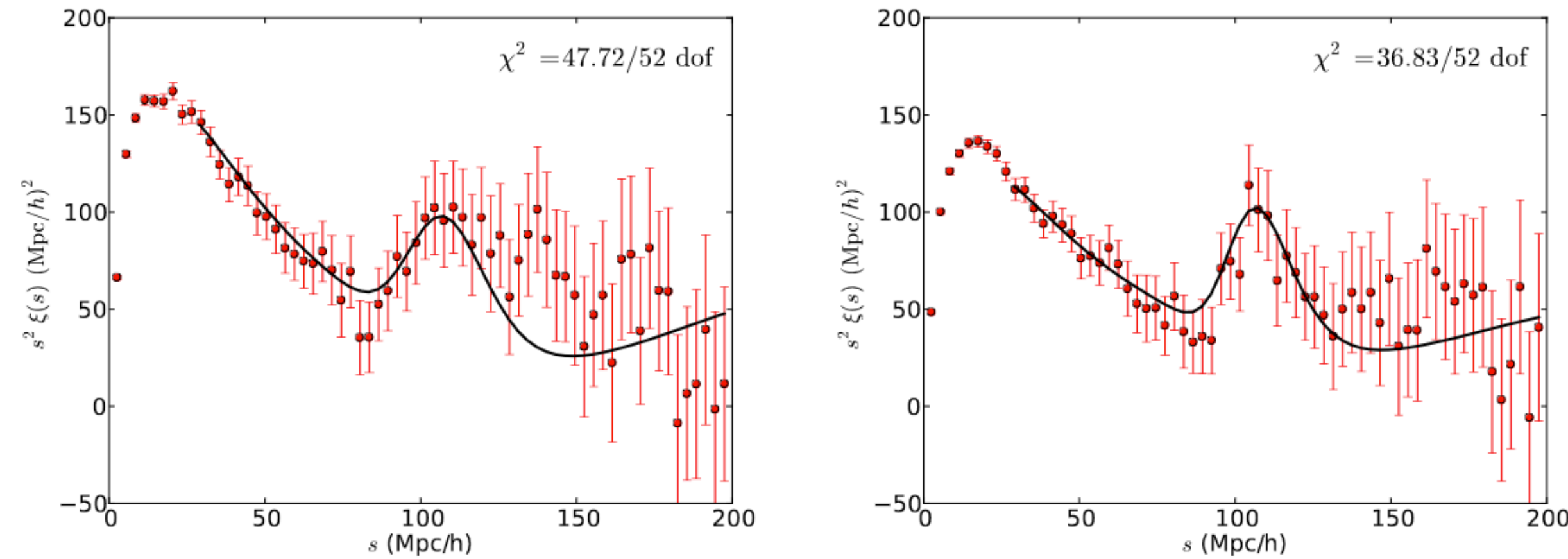
- To enhance the BAO significance, the BAO reconstruction method was proposed by Eisenstein + 2007
- Partially remove the LSS nonlinear evolution and put the particles back to the initial position



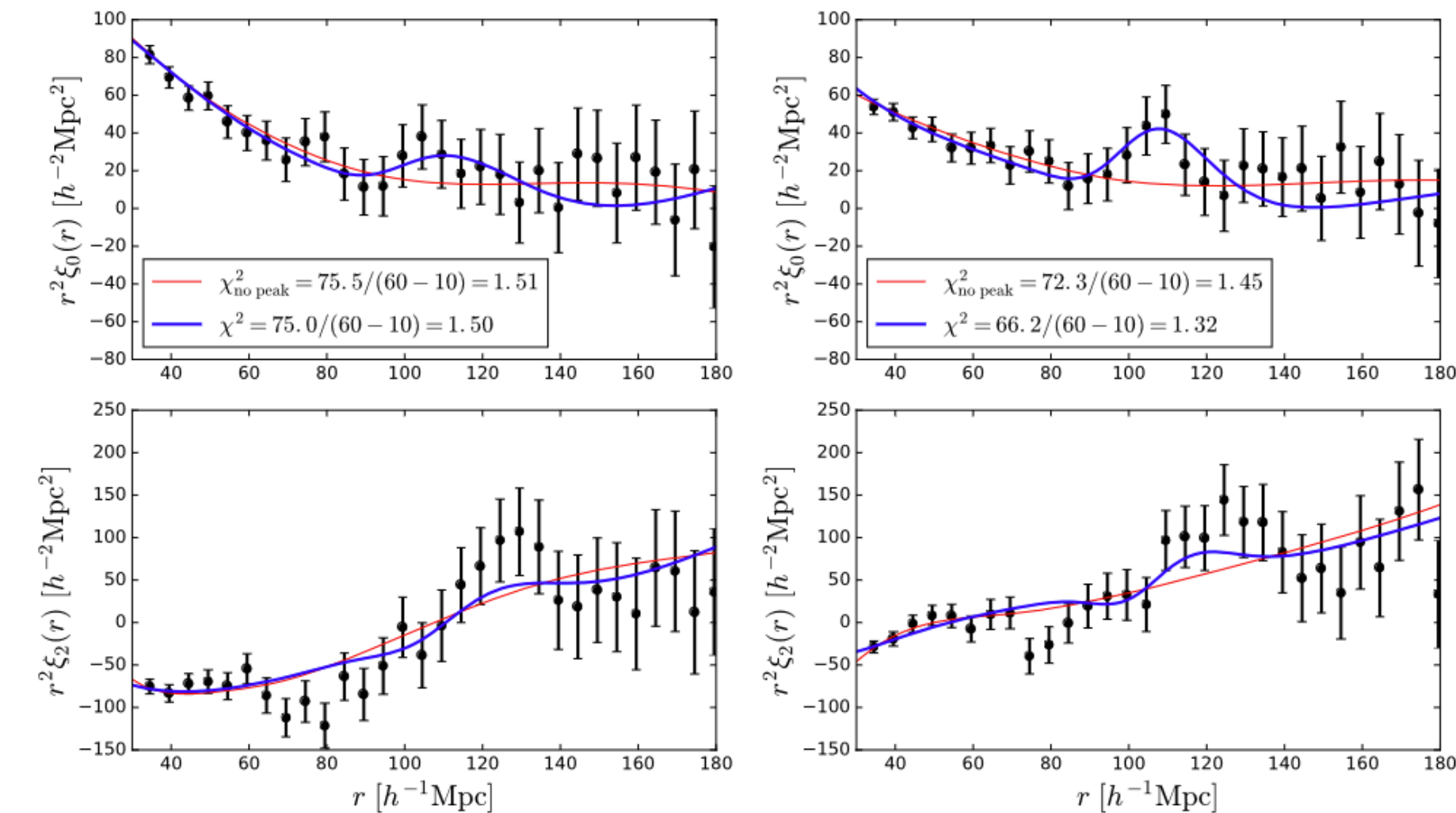
The BAO reconstruction

- routinely applied to spectroscopic BAO analyses, notably SDSS, BOSS, eBOSS

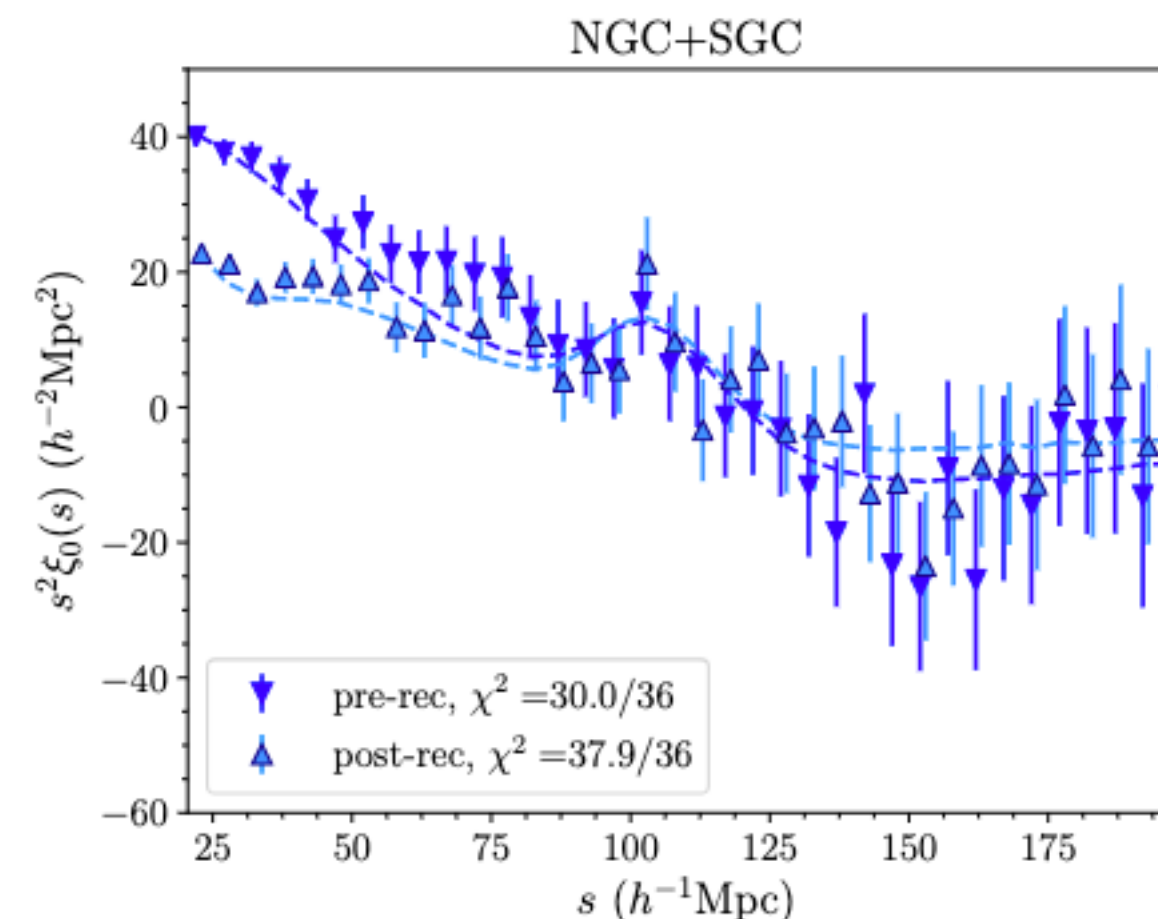
Padmanabhan +, 2012



Alam +, BOSS, 2016



Bautista +, eBOSS LRG, 2018



Raichoor +, eBOSS ELG, 2020

Reconstruction for photometric data?

- Photo-z uncertainties smear most of the radial info
- Unlike RSD, photo-z is a stochastic process
- Reconstruction is effective in transverse direction

True-z

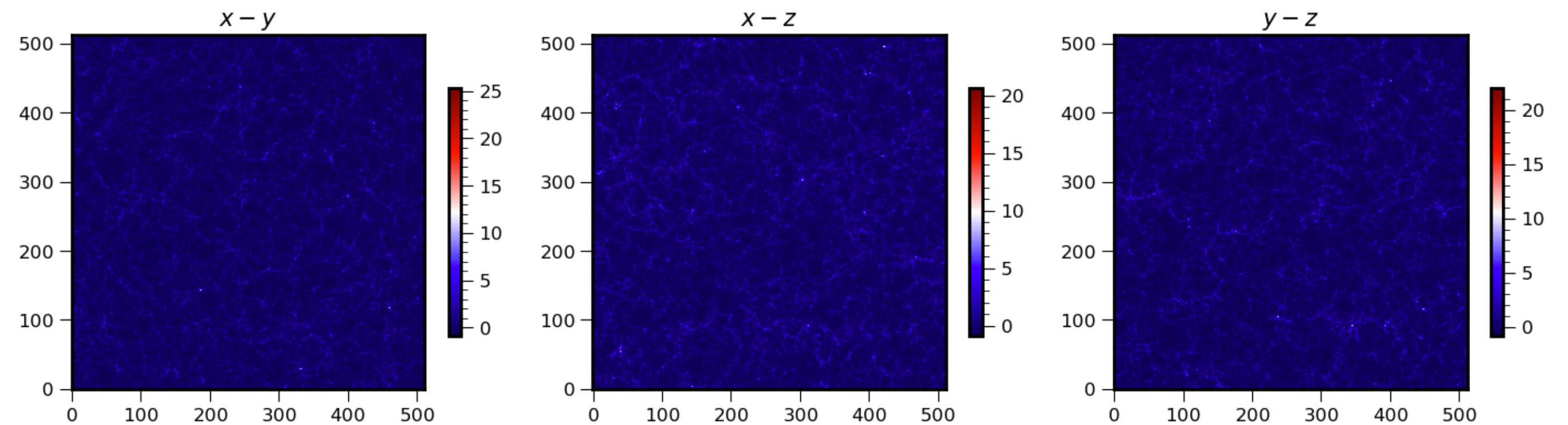
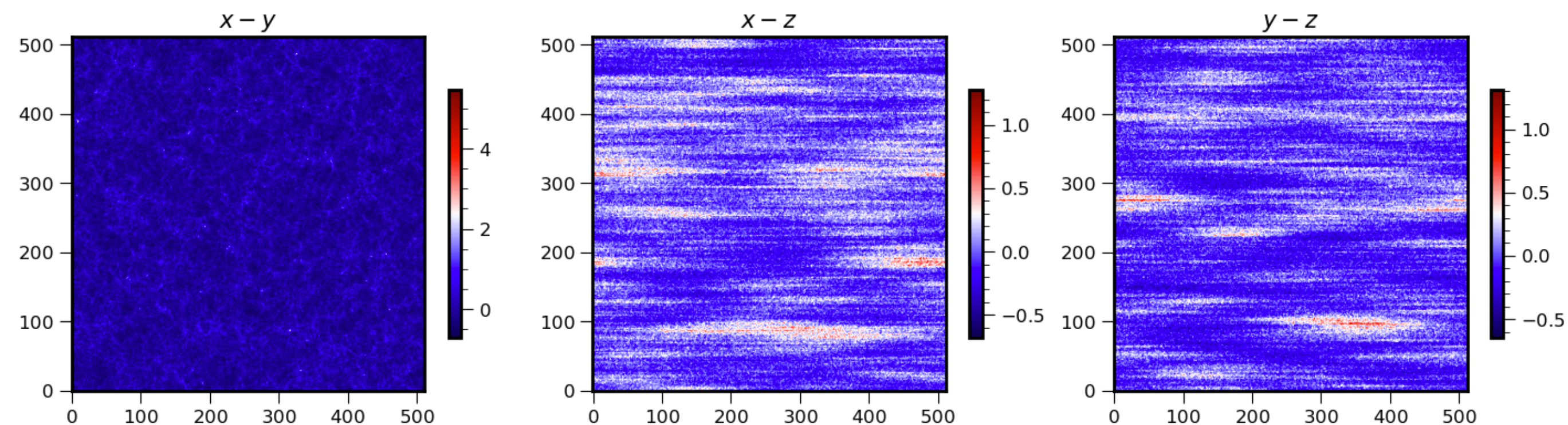


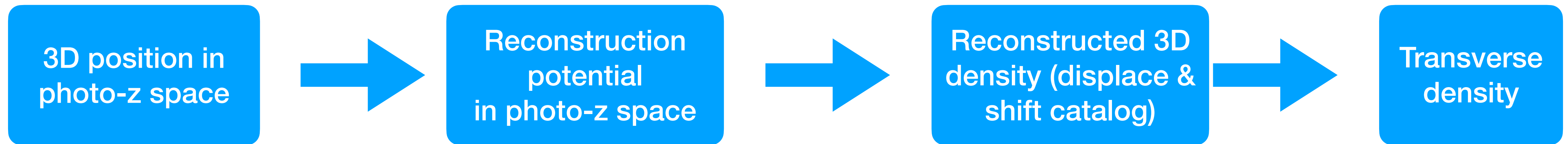
Photo-z



3D photometric BAO reconstruction

- Generalization of the standard ZA reconstruction

$$\nabla^2 \phi_p(\mathbf{x}_\perp, x_\parallel^p) = \delta_p(\mathbf{x}_\perp, x_\parallel^p)$$



**Tomographic bin
projection**

**Directly solve the Poisson eq
in photo-z space**

Unclear how photo-z uncertainties impact the reconstruction results

Transverse potential equation

$$\nabla_{\perp}^2 \phi_p(\mathbf{x}_{\perp}, x_{\parallel}^p) = \delta_p(\mathbf{x}_{\perp}, x_{\parallel}^p) - \frac{\partial^2}{\partial x_{\parallel}^{p2}} \phi_p(\mathbf{x}_{\perp}, x_{\parallel}^p) \quad \nabla_{\perp}^2 \langle \phi_p \rangle(\mathbf{x}_{\perp}) = \langle \delta_p \rangle(\mathbf{x}_{\perp}) - \left\langle \frac{\partial^2}{\partial x_{\parallel}^{p2}} \phi_p(\mathbf{x}_{\perp}, x_{\parallel}^p) \right\rangle$$

Split the field in radial
and transverse direction



Tomographic bin
projection



Reconstruction potential
in transverse space



Reconstructed 2D density
(displace & shift catalog)

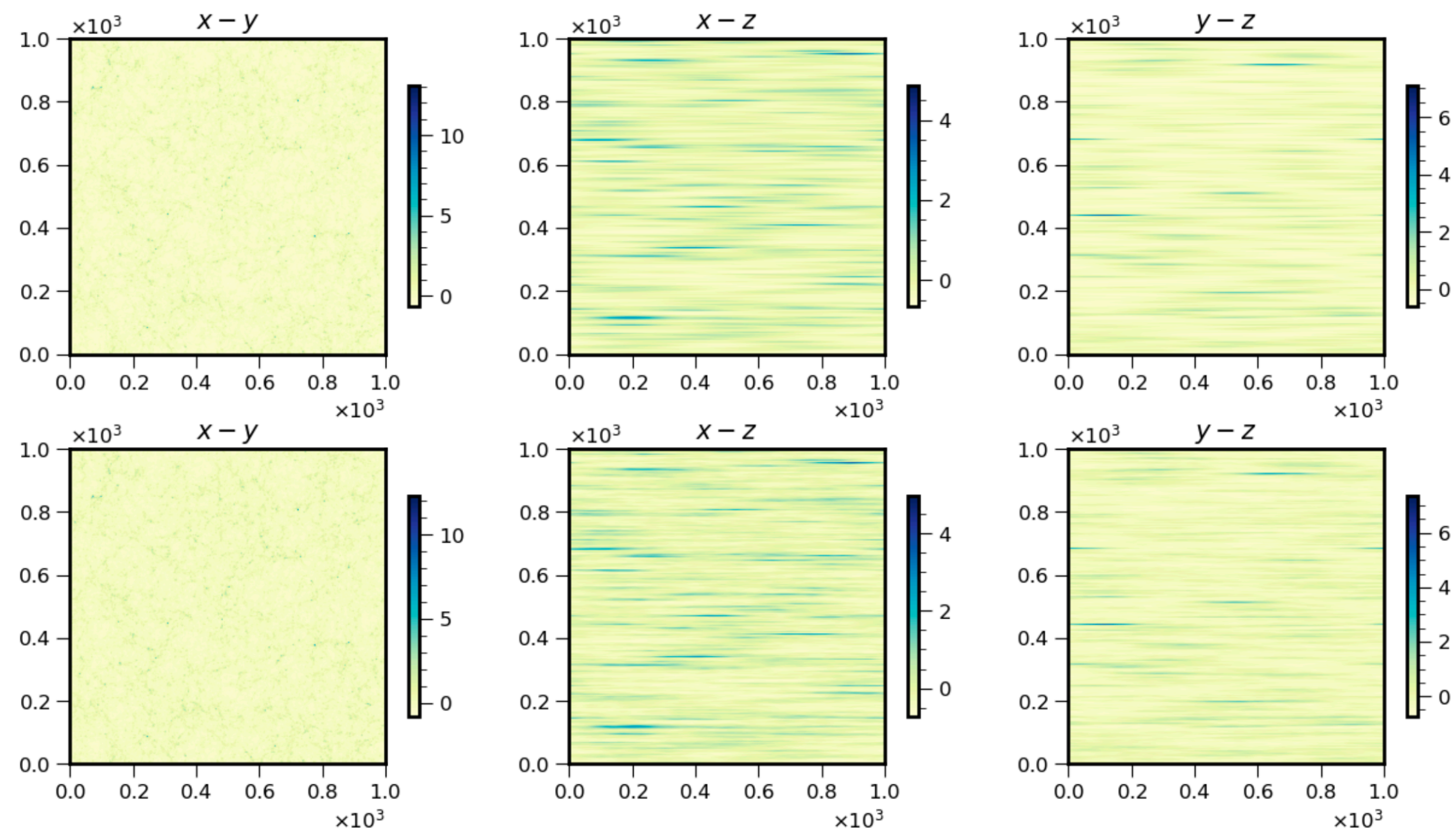
**Additional source to 2D potential
eq. from radial contribution**

- Splitting the field into transverse and radial directions, easy to see the impact of the photo-z

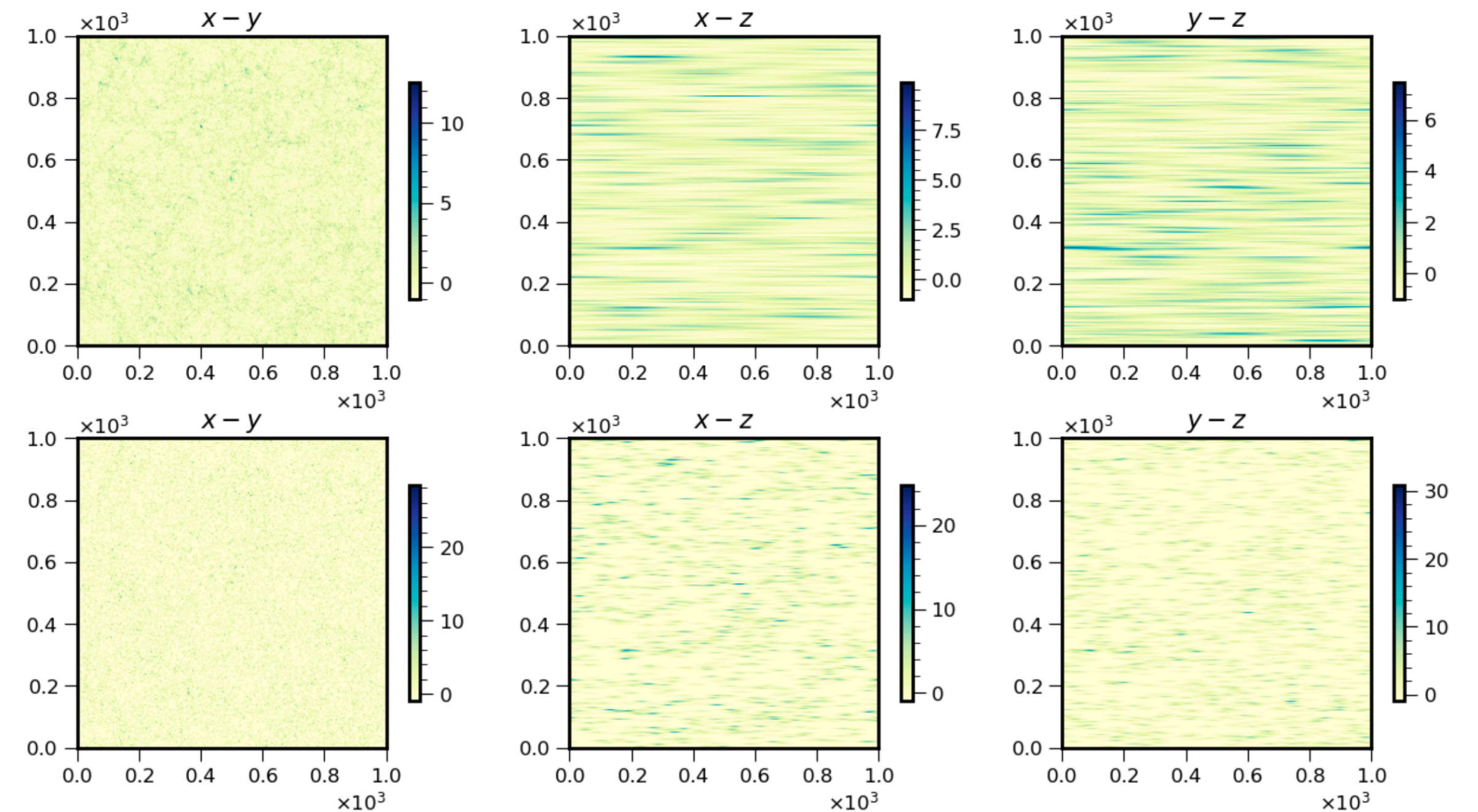
Photo-z stochasticity

- For matter, the effect of stochasticity is weak, but for sparse sample, it is strong

Matter



Halo

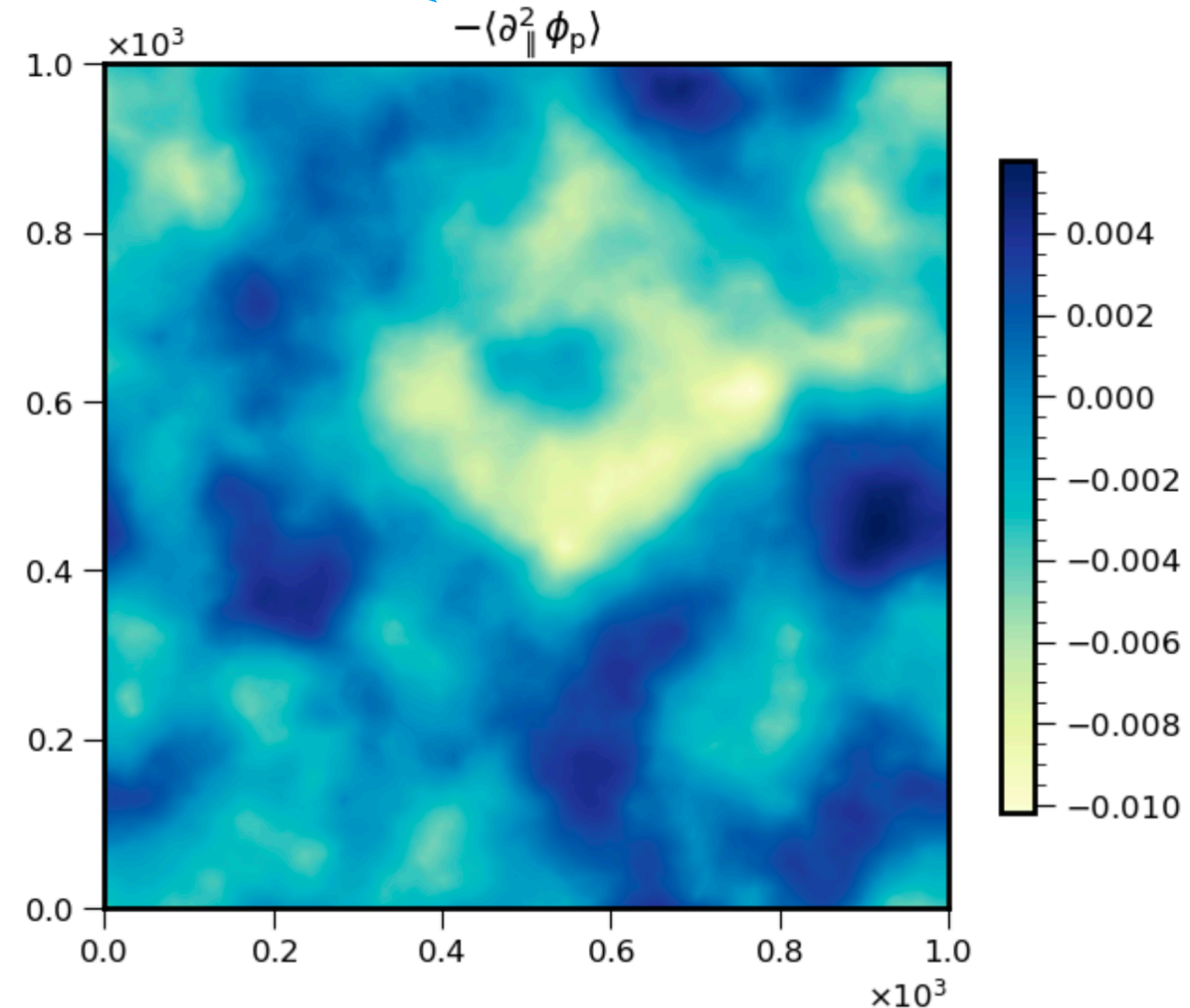
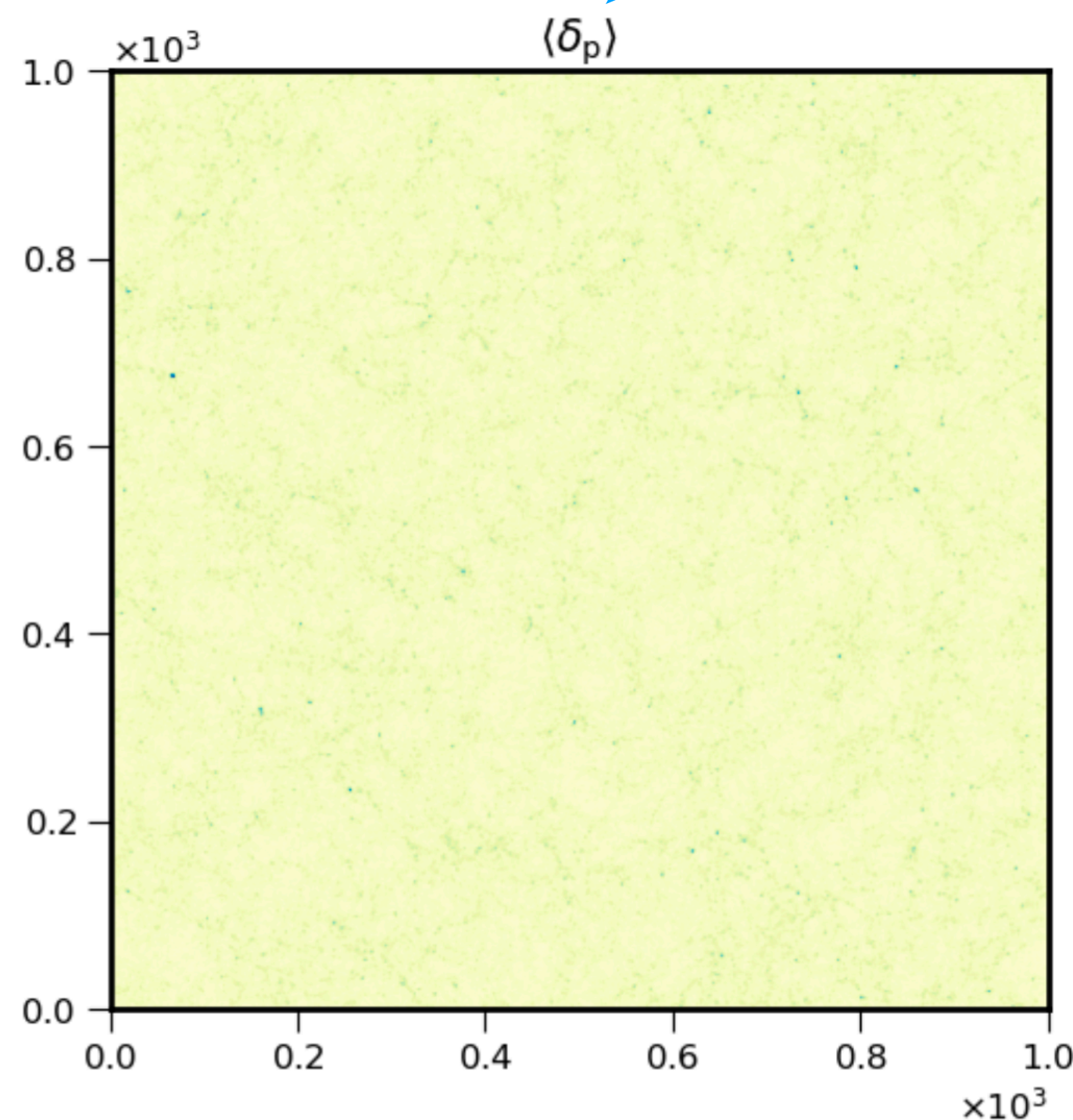


Sources of the transverse potential

- The source contribution is dominated by the density on the slab

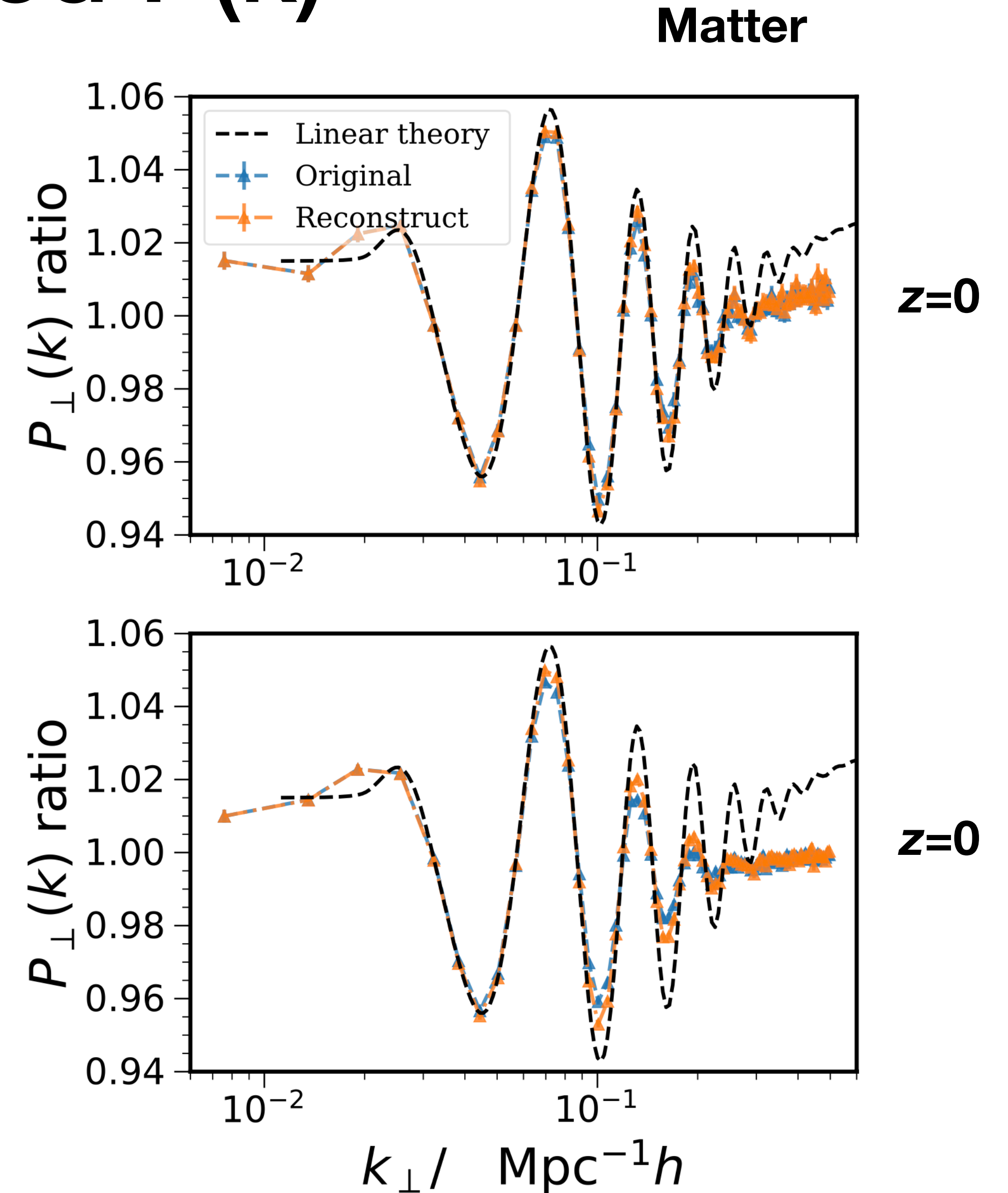
$$\nabla_{\perp}^2 \langle \phi_p \rangle(\mathbf{x}_{\perp}) = \langle \delta_p \rangle(\mathbf{x}_{\perp}) - \left\langle \frac{\partial^2}{\partial x_{\parallel}^2} \phi_p(\mathbf{x}_{\perp}, x_{\parallel}^p) \right\rangle$$

Effectively 2D



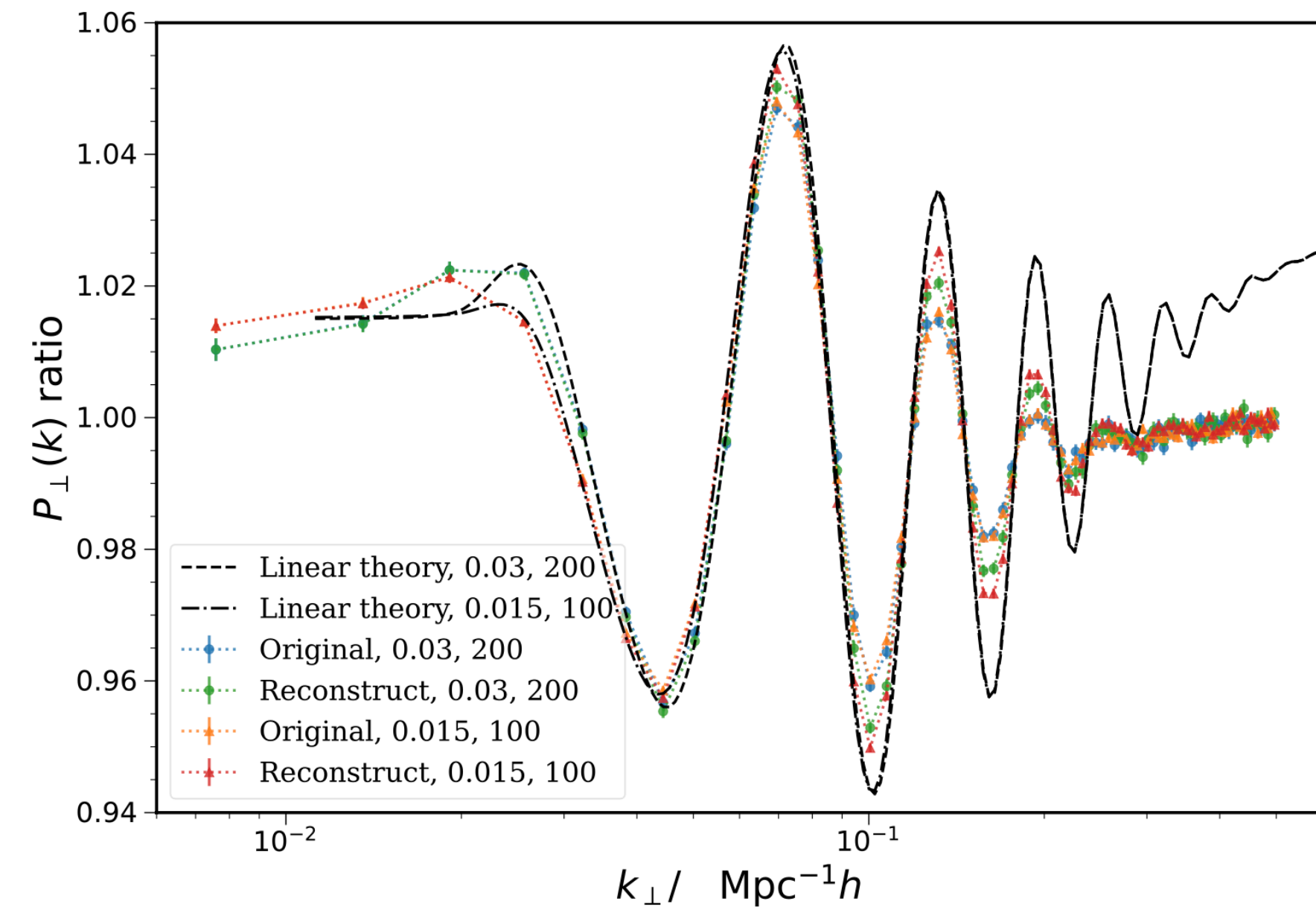
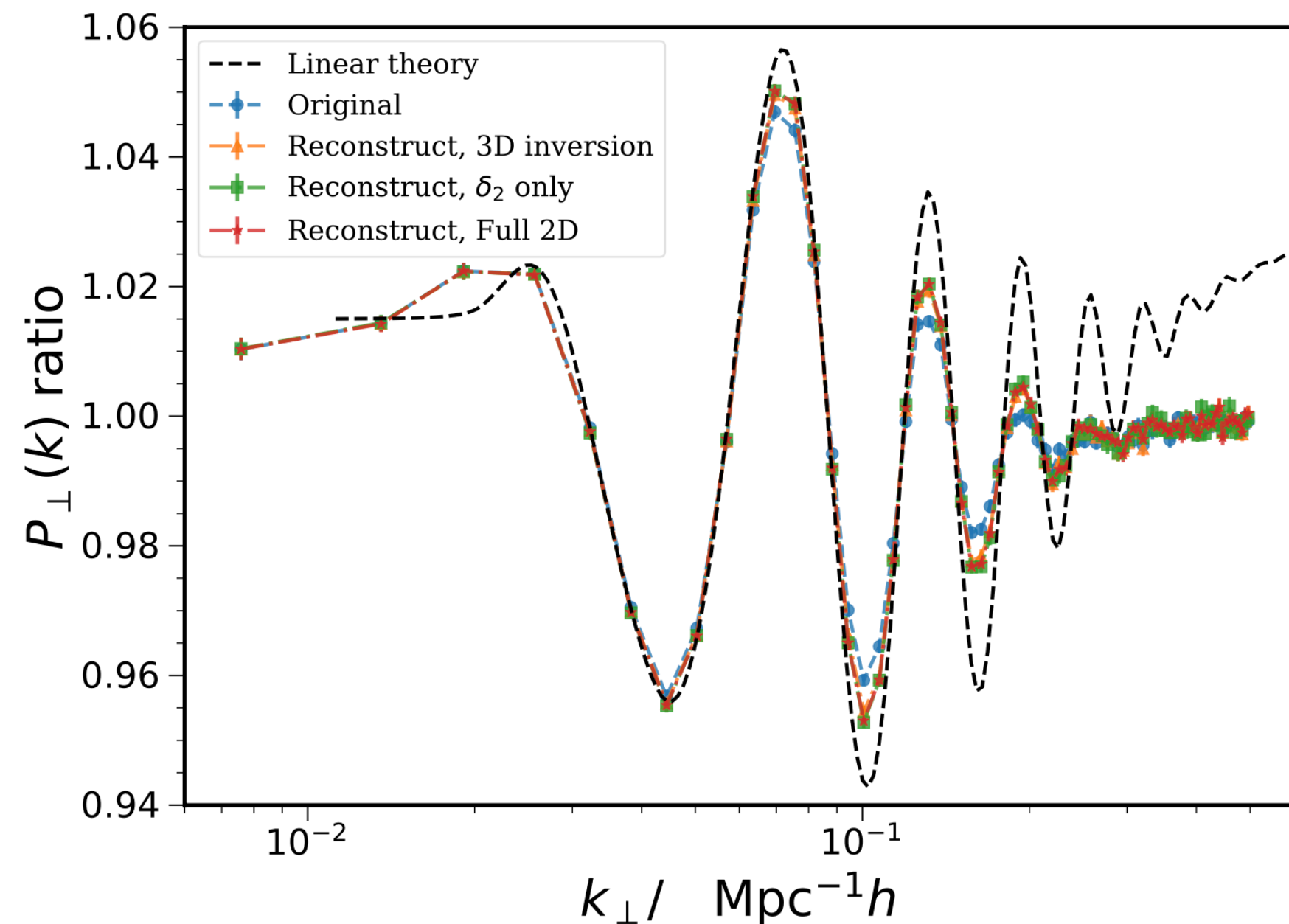
Reconstructed $P(k)$

- The reconstructed power spectrum enhances the BAO feature
- Can be half % level at $z=0$
- The number density of the halo sample is too low to reveal the impact of reconstruction



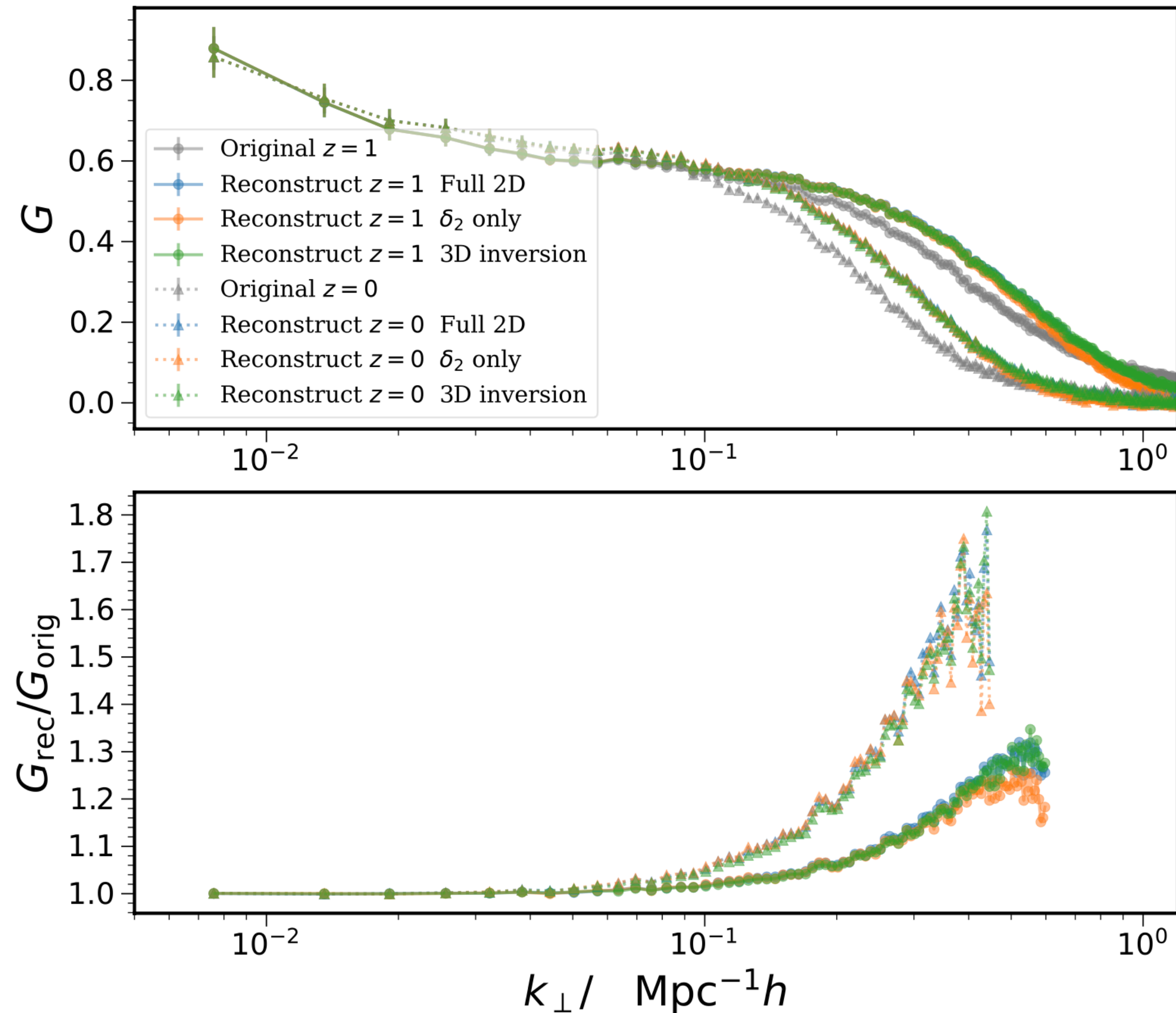
Reconstruction under different conditions

- 3D Poisson inversion, 2D density-only solution, Full 2D solution gives similar results, 2D modeling is sufficient
- For smaller photo-z uncertainties, the enhancement improve



Cross correlation with the initial conditions

- Reconstruction can increase the cross correlation between the final field and the initial conditions (propagator)



Prospects of application to survey data

- Transverse BAO reconstruction can enhance the BAO signals in the data.
- The simple ZA reconstruction strategy can be easily applied to survey data
- BAO reconstruction relies on the number density of the sample (the actual BAO sample number density is much higher than the halo number density here)
- Plan to apply to DES Y6 data.

Conclusions

- DES Y6 use 16 million red galaxies in an area of 4200 deg^2 to measure the photometric BAO.
- Three statistics to applied to measure the transverse BAO, including projective correlation function ξ_p , and yield the most precise photometric BAO measurement
- $D_M(z = 0.87)/r_d = 19.79 \pm 0.42 \text{ [tot.]}$
- Transverse BAO reconstruction can be easily generalized to enhance the significance of the BAO, expected to straightforward application to data.

Backup slides

BAO sample re-optimized

- Run Fisher forecast on gold catalog to find a and b s.t. the BAO error is minimized
- $a=19.64$, $b=2.894$** ($a=19$, $b=3$ in Y3)

$$1.7 < i - z < 2(r - i)$$

$$0.6 < z_{\text{ph}} < 1.2$$

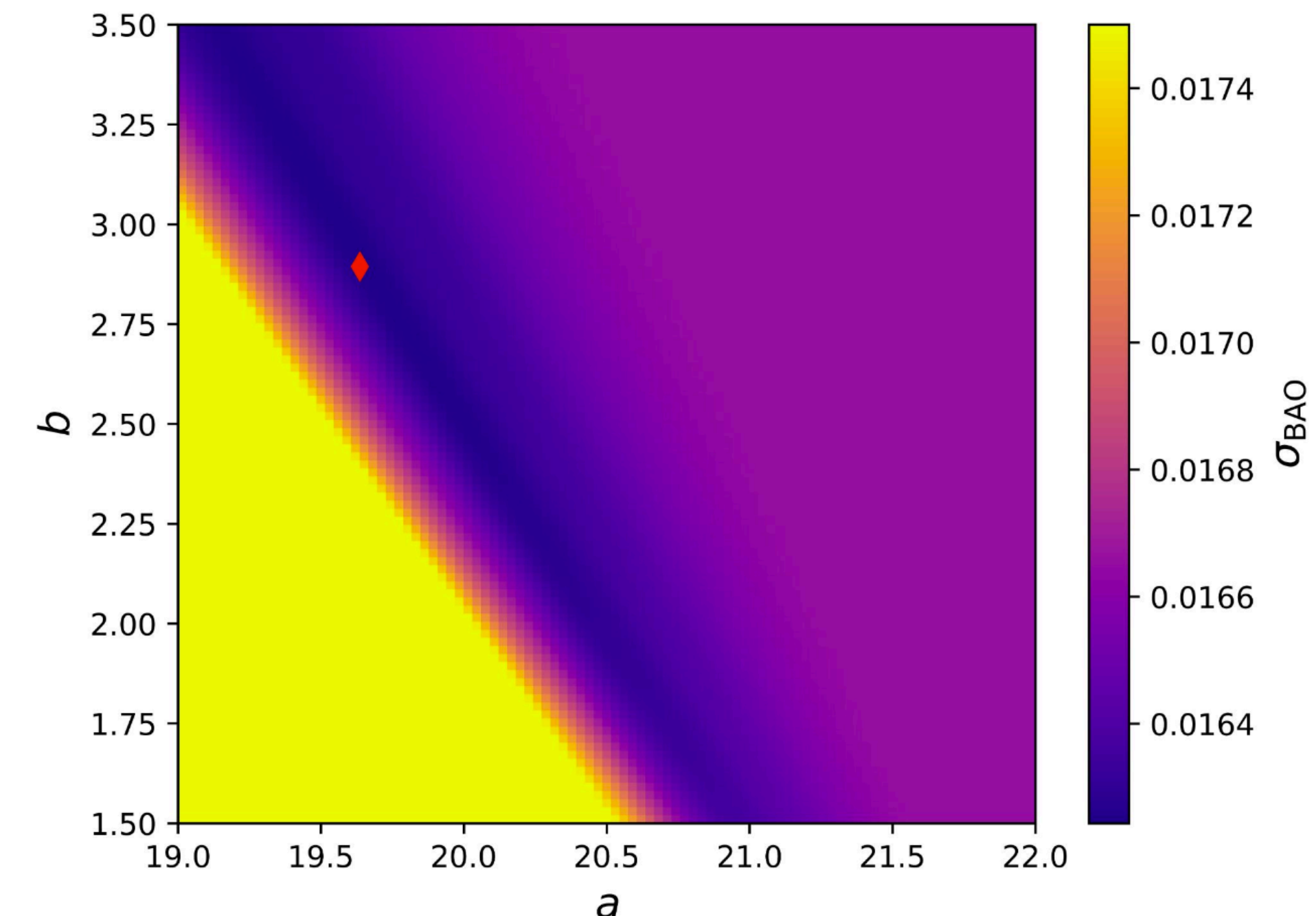
$$i < 22.5$$

$$i < a + bz_{\text{ph}}$$

$$19 \leq a \leq 22, \quad 1.5 \leq b \leq 3.5$$

Case	σ_{BAO}
Y3	0.0214
Y6-Y3sel (5 redshift bins) .	0.0185
Y6-Y3sel (6 redshift bins) .	0.0176
Y6-opt (5 redshift bins) ...	0.0170
Y6-opt (6 redshift bins)	0.0162

Expected to have ~25% improvement in constraint w.r.t Y3

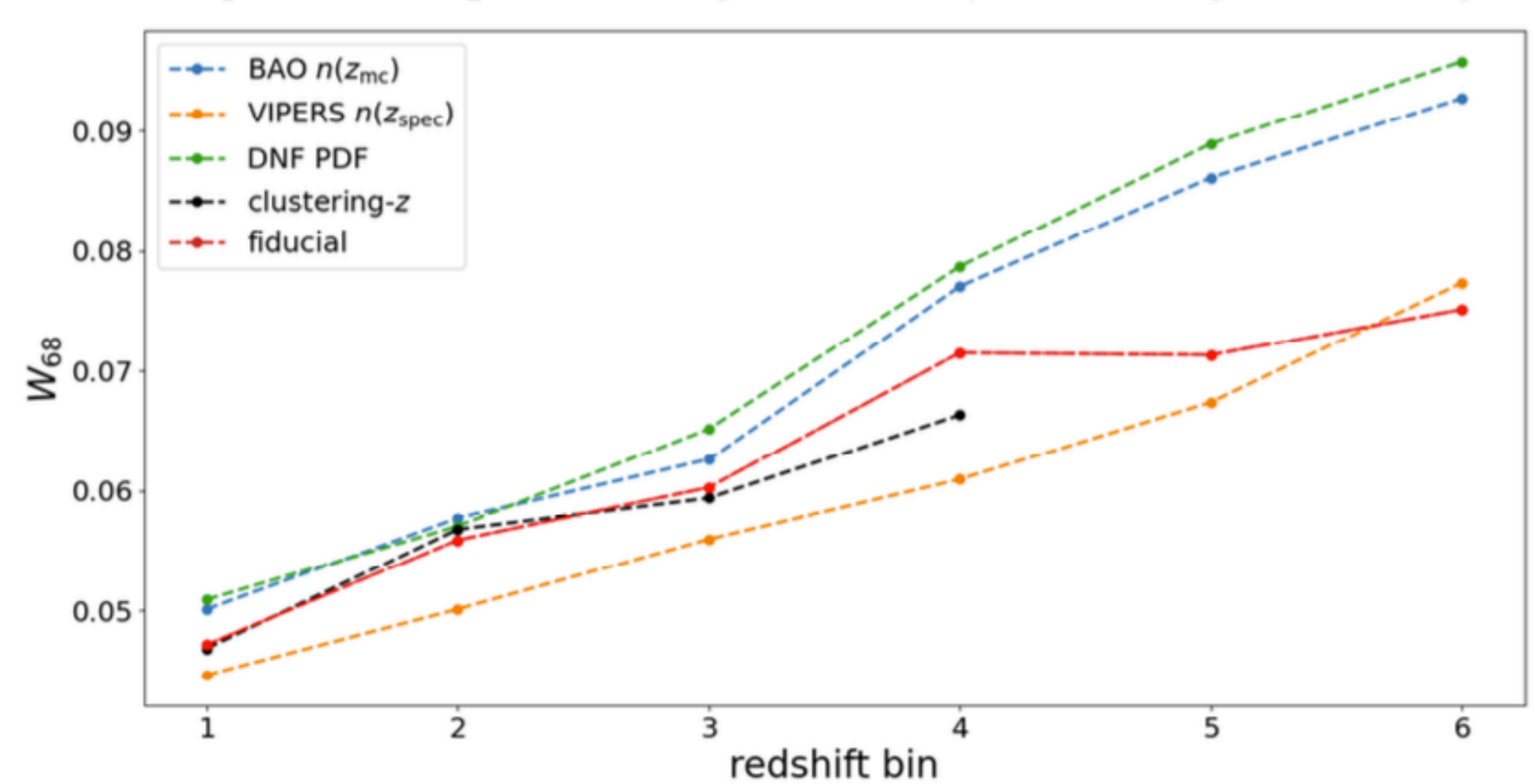
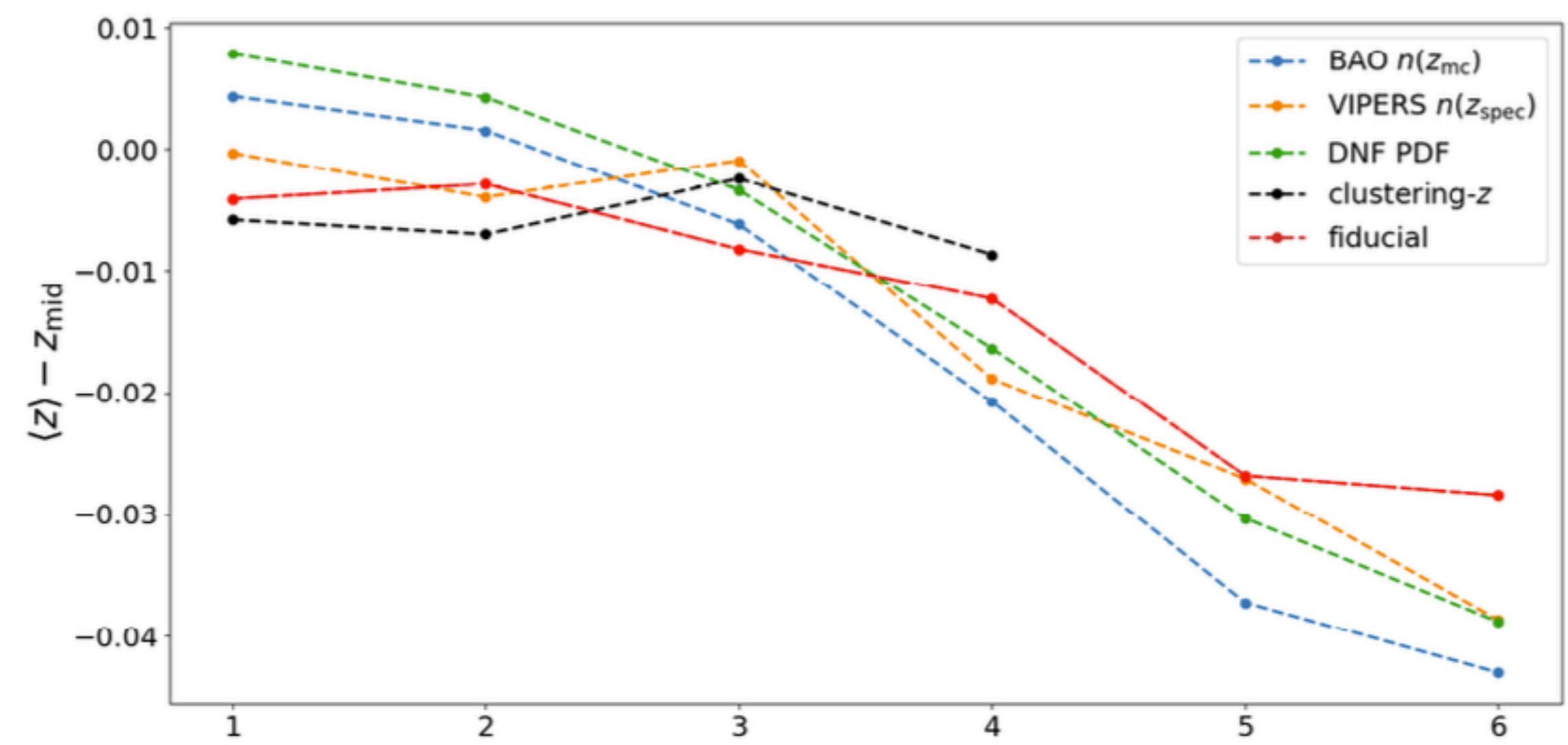


Systematics mitigation

- Iterative Systematics Decontamination (ISD) algorithm: apply weight to each galaxy until the dependence of gal number density on survey properties are not significant
- Five (out of 17) maps are significant, each bin at most three maps needs to be corrected for
- Linear correction is sufficient.
- Systematics give smooth contribution, BAO is insensitive to it

Different true-z distribution estimate

Bin	$\langle z \rangle$					W_{68}						
	DNF	Z_MC	$n(z_{\text{spec}})$	DNF PDF	clustering- z	fiducial	DNF	Z_MC	$n(z_{\text{spec}})$	DNF PDF	clustering- z	fiducial
$0.6 < z_{\text{ph}} < 0.7$	0.654		0.650	0.658	0.644	0.646	0.050		0.045	0.051	0.047	0.047
$0.7 < z_{\text{ph}} < 0.8$	0.752		0.746	0.754	0.743	0.747	0.058		0.050	0.057	0.057	0.056
$0.8 < z_{\text{ph}} < 0.9$	0.844		0.849	0.847	0.848	0.842	0.063		0.056	0.065	0.059	0.060
$0.9 < z_{\text{ph}} < 1.0$	0.929		0.931	0.934	0.941	0.938	0.077		0.061	0.079	0.066	0.071
$1.0 < z_{\text{ph}} < 1.1$	1.013		1.023	1.020	—	1.023	0.086		0.067	0.089	—	0.071
$1.1 < z_{\text{ph}} < 1.2$	1.107		1.111	1.111	—	1.122	0.093		0.077	0.096	—	0.075



Test of photo-z

- Individual bins fit results are consistent
- For bin 6, the bias and error are larger, but its impact on full results is weak

bin	method	fid.	DNF z_{mc}	VIPERS	WZ	DNF PDF
1	ACF	1.000 ± 0.055	0.990 ± 0.055	0.993 ± 0.053	1.001 ± 0.055	0.985 ± 0.056
1	APS	1.0000 ± 0.0617	0.9899 ± 0.0612	0.9927 ± 0.0610	1.0009 ± 0.0623	0.9852 ± 0.0610
1	PCF	0.9998 ± 0.0446	0.9922 ± 0.0458	0.9930 ± 0.0426	0.9994 ± 0.0440	0.9882 ± 0.0460
2	ACF	1.000 ± 0.048	0.992 ± 0.048	0.995 ± 0.046	0.999 ± 0.049	0.992 ± 0.048
2	APS	1.0000 ± 0.0518	0.9920 ± 0.0514	0.9945 ± 0.0512	0.9987 ± 0.0518	0.9924 ± 0.0514
2	PCF	0.9998 ± 0.0426	10.9938 ± 0.0432	0.9954 ± 0.0408	1.0002 ± 0.0426	0.9930 ± 0.0436
3	ACF	1.000 ± 0.042	0.996 ± 0.042	0.992 ± 0.041	0.999 ± 0.042	0.995 ± 0.043
3	APS	1.0000 ± 0.0438	0.9957 ± 0.0438	0.9914 ± 0.0435	0.9991 ± 0.0440	0.9954 ± 0.0439
3	PCF	0.9998 ± 0.0412	0.9982 ± 0.0418	0.9942 ± 0.0392	0.9994 ± 0.0406	0.9970 ± 0.0426
4	ACF	1.000 ± 0.041	1.002 ± 0.042	1.011 ± 0.040	0.998 ± 0.040	1.003 ± 0.043
4	APS	1.0000 ± 0.0402	1.0017 ± 0.0408	1.0106 ± 0.0405	0.9981 ± 0.0403	1.0025 ± 0.0408
4	PCF	0.9998 ± 0.0404	1.0026 ± 0.0422	1.0082 ± 0.0390	1.0010 ± 0.0388	1.0026 ± 0.0428
5	ACF	1.000 ± 0.047	1.003 ± 0.049	0.999 ± 0.045	—	0.999 ± 0.052
5	APS	1.0000 ± 0.0401	1.0030 ± 0.0409	0.9971 ± 0.0402	—	0.9995 ± 0.0410
5	PCF	0.9994 ± 0.0446	1.0018 ± 0.0509	1.0026 ± 0.0434	—	0.9978 ± 0.0507
6	ACF	1.000 ± 0.068	1.006 ± 0.074	1.005 ± 0.070	—	1.001 ± 0.077
6	APS	1.0000 ± 0.0458	1.0067 ± 0.0475	1.0047 ± 0.0466	—	1.0022 ± 0.0469
6	PCF	0.9998 ± 0.0831	1.0130 ± 0.0941	1.0234 ± 0.0773	—	1.0078 ± 0.0985
All	ACF	1.000 ± 0.020	0.997 ± 0.021	0.999 ± 0.019	—	0.996 ± 0.021
All	APS	1.0000 ± 0.0190	0.9988 ± 0.0194	0.9989 ± 0.0192	—	0.9971 ± 0.0193
All	PCF	0.9998 ± 0.0202	0.9982 ± 0.0214	1.0002 ± 0.0196	—	0.9962 ± 0.0216

Detection of BAO

- BAO signals are detected in individual bins, except the first bin (same in Y3)

Bin	ACF	APS	PCF
All	99.95 % [Y]	99.49 % [Y]	100 % [Y]
1	90.32 % [N]	74.49 % [N]	95.39 % [N]
2	94.98 % [Y]	82.12 % [Y]	97.34 % [Y]
3	97.39 % [Y]	86.73 % [Y]	97.69 % [Y]
4	97.59 % [Y]	91.55 % [Y]	97.84 % [Y]
5	96.67 % [Y]	90.73 % [Y]	95.39 % [Y]
6	91.19 % [Y]	87.76 % [Y]	86.22 % [Y]
Non-detections			
0	72.90 %	41.80 %	73.77 %
1	22.85 %	36.42 %	22.69 %
2	3.84 %	16.03 %	3.23 %
3	0.31 %	4.82 %	0.26 %
4	0.10 %	0.92 %	0.05 %

Pre-unblinding tests on individual methods: **passed**

- Tests on the normality of the data while conforming to the blinding protocol
- Single failure of the test observed for ACF and APS, well within the expectation from mocks

ACF

Threshold (Fraction of mocks)	90 %		95 %		97 %		99 %		data	
	min	max	min	max	min	max	min	max	MICE	Planck
	$10^2(\alpha - \alpha_{\text{fiducial}})$									
Bins 23456	-1.33	1.43	-1.79	1.86	-2.10	2.17	-2.44	2.76	0.77	1.12
Bins 13456	-1.39	1.63	-1.83	1.99	-2.03	2.30	-2.80	3.13	1.02	1.39
Bins 12456	-1.37	1.51	-1.71	2.00	-2.03	2.35	-2.52	3.23	-0.25	-0.46
Bins 12356	-1.45	1.27	-1.81	1.57	-2.19	1.88	-2.80	2.76	-0.66	-0.31
Bins 12346	-1.21	1.11	-1.51	1.41	-1.79	1.72	-2.48	2.02	0.39	0.47
Bins 12345	-0.86	0.76	-1.07	0.96	-1.30	1.15	-1.63	1.65	-0.69	-0.84
Bins 456	-2.85	3.73	-3.42	4.85	-3.86	5.54	-5.00	7.90	3.17	3.28
Bins 123	-3.30	2.65	-4.27	3.45	-5.04	4.26	-6.80	5.56	-1.54	-1.59
Bins 1234	-1.83	1.67	-2.25	2.13	-2.55	2.35	-3.67	3.22	-0.38	-0.77
Template Cosmo	-0.33	0.48	-0.40	0.60	-0.44	0.68	-0.55	0.89	x	0.22
Covariance	-0.46	0.42	-0.58	0.54	-0.68	0.64	-0.83	0.82	x	-0.48
$n(z)$ z_{mc} -fid	-0.56	0.08	-0.60	0.14	-0.64	0.20	-0.72	0.31	x	-0.48
	$100(\sigma - \sigma_{\text{All Bins}})/\sigma_{\text{All Bins}}$									
Bins 23456	-2.47	25.15	-4.33	30.34	-6.09	35.42	-9.08	41.50	5.83	3.06
Bins 13456	-1.60	26.16	-3.55	31.21	-5.18	35.18	-8.95	45.61	18.45	13.97
Bins 12456	-2.00	26.22	-4.53	31.44	-5.84	36.80	-8.93	45.86	17.48	14.85
Bins 12356	-2.29	25.17	-4.09	30.79	-5.51	35.11	-9.35	41.35	8.74	4.37
Bins 12346	-1.39	19.89	-2.84	24.51	-4.07	27.92	-6.22	34.80	7.77	7.42
Bins 12345	-0.66	11.94	-1.45	14.87	-1.97	17.79	-3.56	22.50	0.49	-3.06
Bins 456	12.08	94.25	8.20	114.76	5.13	128.50	-1.76	166.46	65.05	56.33
Bins 123	10.14	80.86	5.92	95.62	3.02	109.42	-2.36	144.43	22.82	18.34
Bins 1234	1.37	35.50	-0.99	42.58	-1.84	45.70	-4.23	55.74	7.77	4.80

APS

Threshold (Fraction of mocks)	0.9		0.95		0.97		0.99		data	
	min	max	min	max	min	max	min	max	MICE	Planck
	$10^2(\alpha - \alpha_{\text{fiducial}})$									
Bins 23456	-1.18	1.45	-1.59	1.85	-2.01	2.12	-2.99	3.19	0.24	0.54
Bins 13456	-1.46	1.55	-1.88	2.26	-2.24	2.76	-3.54	3.60	1.44	1.76
Bins 12456	-1.32	1.48	-1.82	2.07	-2.14	2.71	-2.75	4.22	-0.22	-0.29
Bins 12356	-1.55	1.28	-2.05	1.79	-2.63	2.10	-4.36	3.08	-0.21	-0.22
Bins 12346	-1.48	1.43	-2.01	1.91	-2.67	2.49	-3.96	3.31	1.22	0.65
Bins 12345	-1.59	1.45	-2.10	2.00	-2.67	2.42	-3.95	3.60	-1.50	-1.39
Bins 456	-2.68	3.75	-3.25	4.91	-4.08	5.56	-5.96	8.06	2.31	3.25
Bins 123	-4.58	3.44	-6.16	4.46	-7.80	5.49	-14.48	7.00	-1.32	-1.83
Bins 1234	-2.78	2.47	-3.87	3.37	-4.58	4.29	-6.38	6.17	-0.79	-1.13
Template Cosmo	-0.59	0.62	-0.72	0.83	-0.89	0.99	-1.20	1.60	x	-0.49
Covariance	-0.57	0.62	-0.75	0.79	-0.91	0.91	-1.30	1.38	x	-0.09
$n(z)$	-0.35	0.61	-0.47	0.69	-0.55	0.75	-0.78	0.89	x	-0.20
	$100(\sigma - \sigma_{\text{All Bins}})/\sigma_{\text{All Bins}}$									
Bins 23456	-5.53	28.15	-7.91	34.95	-10.77	44.11	-16.41	61.14	-1.43	0.72
Bins 13456	-5.06	33.65	-8.46	40.63	-11.21	47.60	-18.61	78.34	13.66	18.11
Bins 12456	-5.09	29.11	-8.63	37.93	-10.67	45.63	-15.98	54.38	24.22	21.10
Bins 12356	-6.17	33.22	-9.39	45.05	-12.03	49.74	-22.23	62.51	8.37	10.48
Bins 12346	-5.67	31.74	-9.73	41.92	-12.71	47.79	-19.20	73.87	13.52	12.11
Bins 12345	-4.89	30.92	-7.90	42.62	-10.77	52.16	-18.77	75.55	-6.10	-7.55
Bins 456	-0.98	97.42	-7.16	130.80	-12.08	155.71	-18.40	203.90	46.17	53.50
Bins 123	1.81	126.95	-3.37	160.80	-7.36	189.98	-17.54	257.44	24.42	16.35
Bins 1234	-3.89	70.89	-7.83	86.84	-12.27	104.47	-22.21	156.87	7.86	1.54

PCF

Threshold (Fraction of mocks)	0.9		0.95		0.97		0.99		data	
	min	max	min	max	min	max	min	max	MICE	Planck
	$10^2(\alpha - \alpha_{\text{fiducial}})$									
Bins 23456	-1.72	1.48	-2.12	1.92	-2.32	2.12	-2.96	2.77	0.88	0.96
Bins 13456	-1.48	1.32	-1.86	1.72	-2.12	1.92	-2.65	2.63	-0.32	-0.20
Bins 12456	-1.28	1.28	-1.64	1.70	-2.00	2.04	-2.53	2.89	0.16	0.24
Bins 12356	-1.16	1.16	-1.46	1.60	-1.68	1.92	-2.57	2.37	-0.48	-0.56
Bins 12346	-0.76	0.96	-1.00	1.20	-1.16	1.52	-1.60	2.00	0.20	0.24
Bins 12345	-0.44	0.52	-0.60	0.64	-0.68	0.72	-0.85	0.88	-0.24	-0.28
Bins 456	-3.76	3.24	-4.85	4.28	-5.40	4.88	-6.59	6.47	2.28	2.32
Bins 123	-1.92	2.44	-2.48	3.12	-2.96	3.52	-4.35	4.36	-1.04	-1.44
Bins 1234	-1.00	1.32	-1.28	1.66	-1.52	1.88	-1.94	2.48	-0.08	-0.12
Template Cosmo	-0.80	0.92	-1.01	1.12	-1.13	1.20	-1.49	1.49	x	0.13
Covariance	-0.40	0.48	-0.48	0.60	-0.56	0.68	-0.73	0.84	x	-0.12
$n(z)$ z_{mc} -fid	-0.40	-0.08	-0.44	-0.04	-0.44	0.00	-0.49	0.04	x	-0.27
	$100(\sigma - \sigma_{\text{All Bins}})/\sigma_{\text{All Bins}}$									
Bins 23456	-1.12	32.11	-3.30	40.01	-4.62	45.33	-6.56	55.20	3.23	4.97
Bins 13456	-1.12	27.14	-2.80	32.06	-3.99	37.51	-6.23	47.73	18.28	16.57
Bins 12456	-1.97	23.91	-3.41	28.78	-4.54	33.69	-6.91	40.64	10.75	6.95
Bins 12356	-1.02	22.99	-2.61	27.89	-3.21	33.89	-5.85	40.96	6.45	7.95
Bins 12346	0.00	15.35	-1.49	18.40	-2.20	20.89	-3.80	26.56	7.53	9.60
Bins 12345	0.00	7.00	-1.14	8.93	-1.34	10.48	-2.12	12.19	2.15	1.32
Bins 456	18.11	124.49	14.14	150.21	10.89	169.93	5.18	222.60	67.74	50.00
Bins 123	6.09	58.36	4.35	69.50	2.92	75.66	-1.03	94.05	22.58	27.15
Bins 1234	8.46	19.08	0.00	26.12	-0.97	29.96	-2.36	37.06	8.60	11.59

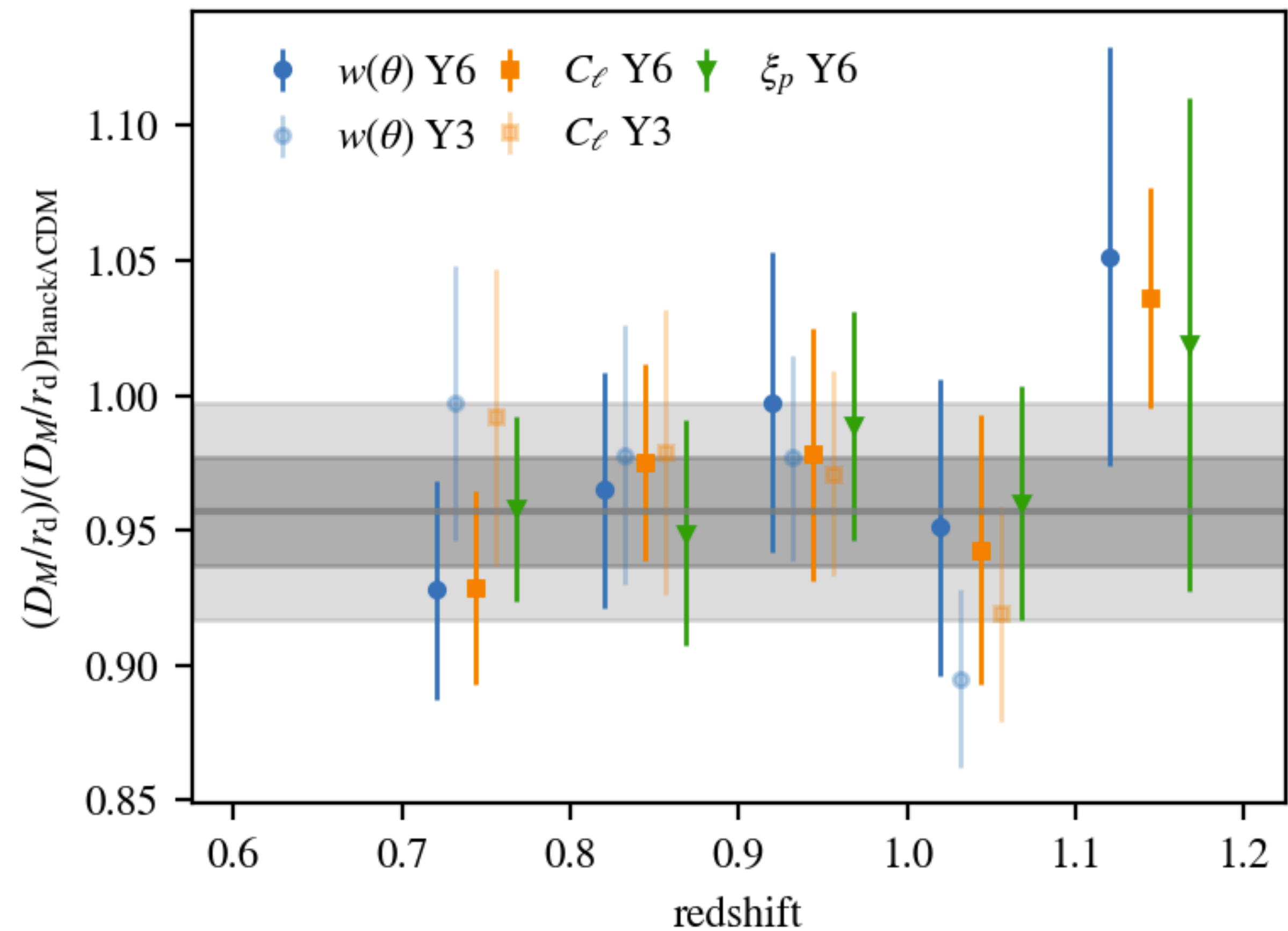
Pre-unblinding tests on combination of the estimators: **passed**

- The measurements from individual method and their combinations are consistent with mock results

$\Delta\alpha \times 100$	Data	90%-mocks
ACF-APS	-0.86	[-1.36, 1.12]
ACF-PCF	-0.11	[-0.58, 1.51]
APS-PCF	0.75	[-1.04, 2.15]
ACF-{APS+PCF}	-0.25	[-0.52, 1.24]
APS-{ACF+PCF}	0.76	[-1.02, 2.02]
PCF-{ACF+APS}	-0.11	[-1.58, 0.61]
AVG-ACF	0.29	[-1.34, 0.58]
AVG-APS	-0.57	[-1.78, 0.81]
AVG-PCF	0.19	[-0.23, 0.39]

Y3 and Y6 comparison

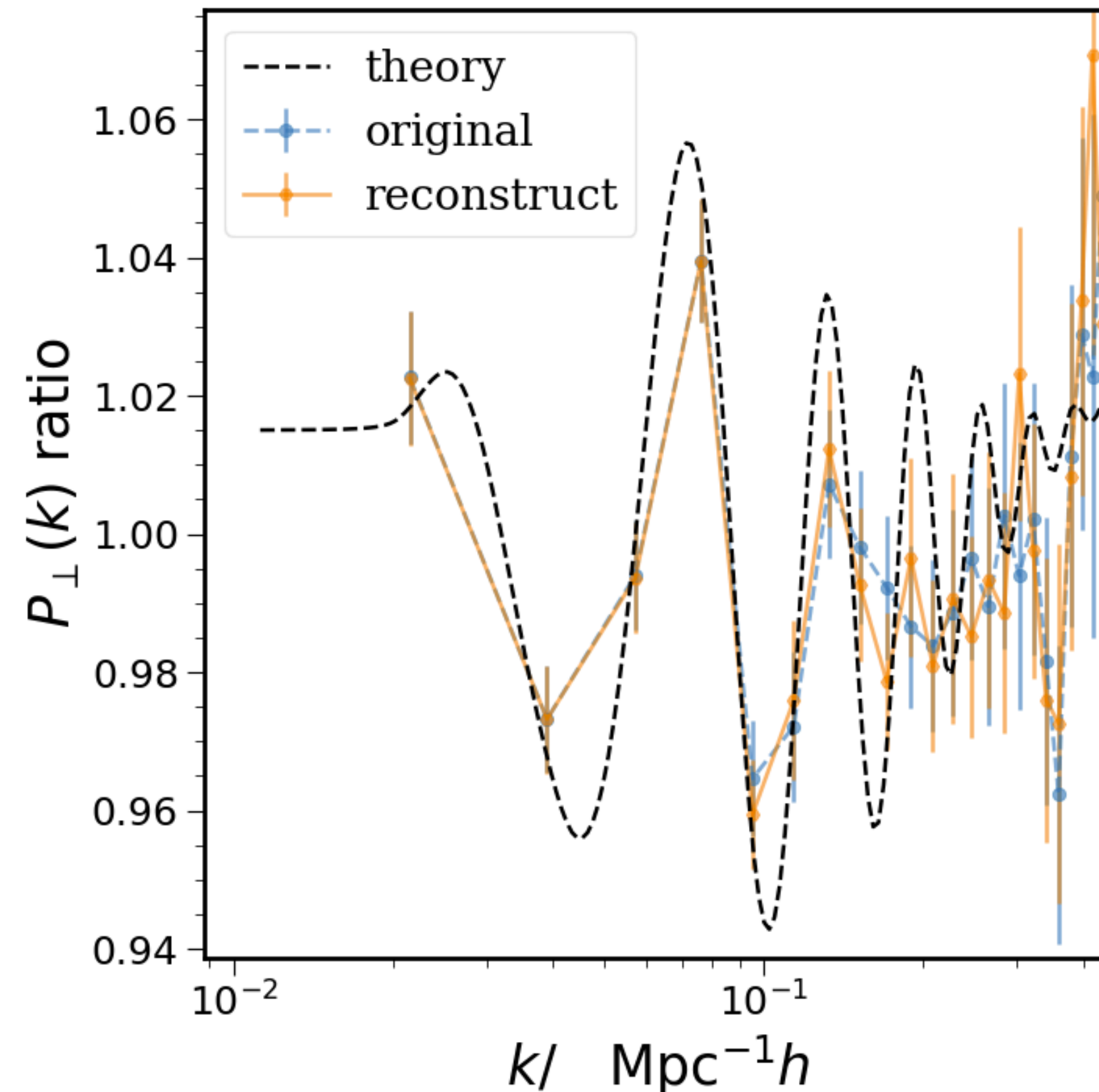
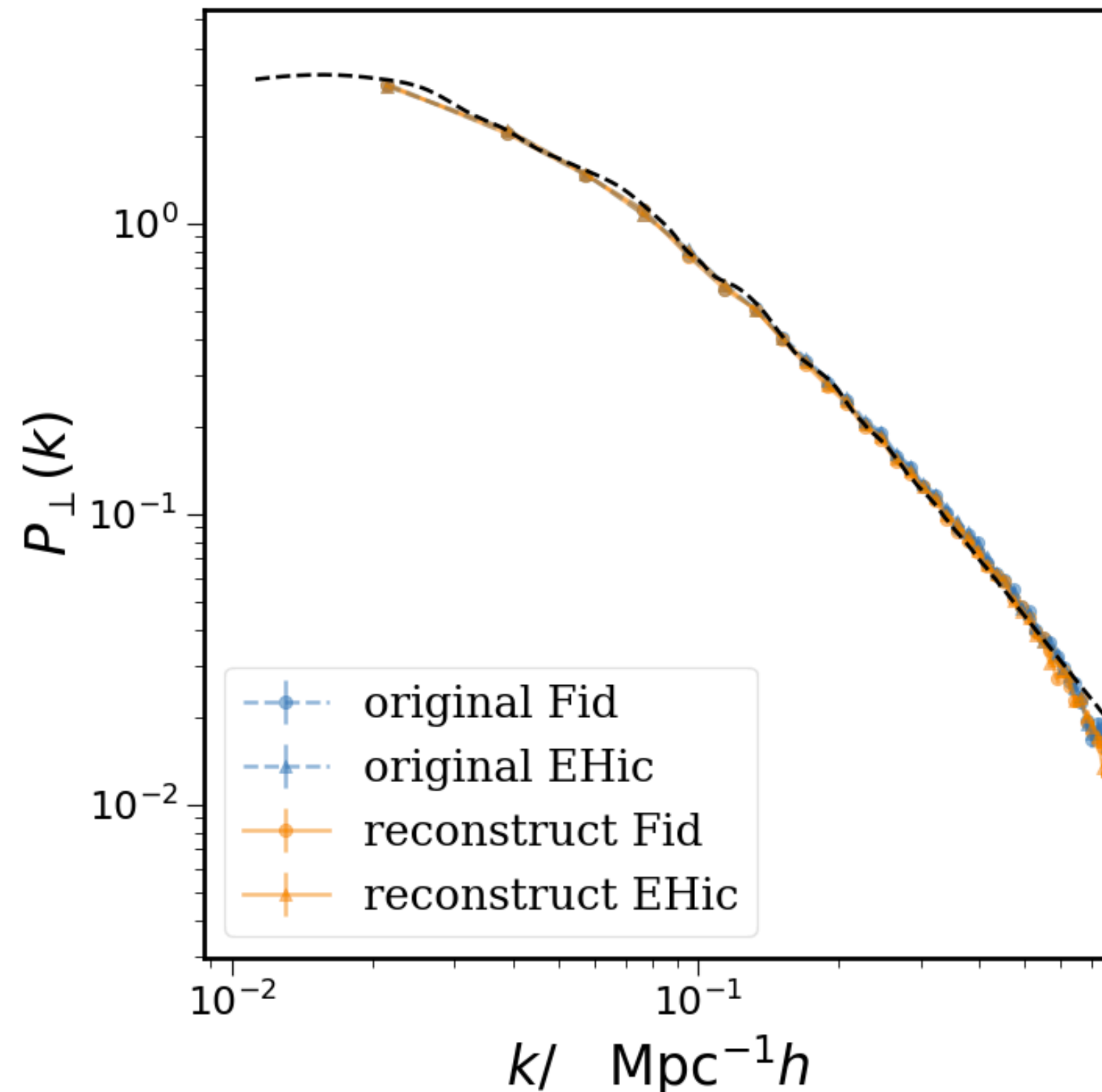
- 38% of Y6 galaxies are also in Y3
- The difference btw Y3 and Y6 are statistically consistent



Reconstructed P(k)

- Although the halo results are much noisier, increase in BAO feature is still visible

Halo $z=0$, mean halo mass $5 \times 10^{13} M_{\odot} h^{-1}$, $n_{\text{den}} = 4 \times 10^{-4} (\text{Mpc} h^{-1})^{-3}$



Correlation of the displacement field

- The correlation of the photometric displacement is much lower than the

